

**STUDY OF FACTORS AFFECTING PRECIPITATE FORMATION IN PALM OIL
BIODIESEL**

VLADIMIR PLATA CHÁVEZ

**UNIVERSIDAD INDUSTRIAL DE SANTANDER
FACULTY OF PHYSICOCHEMICAL ENGINEERINGS
SCHOOL OF CHEMICAL ENGINEERING
DOCTORATE IN CHEMICAL ENGINEERING
BUCARAMANGA**

2015

**STUDY OF FACTORS AFFECTING PRECIPITATE FORMATION IN PALM OIL
BIODIESEL**

VLADIMIR PLATA CHÁVEZ

**Submitted to the School of Chemical Engineering of
Universidad Industrial de Santander
in partial fulfillment to the requirements for the degree of
Doctor en Ingeniería Química**

SUPERVISORS

**Dr. Sc. Viatcheslav Kafarov
Ph.D. María Paola Maradei García
Universidad Industrial de Santander**

**UNIVERSIDAD INDUSTRIAL DE SANTANDER
FACULTY OF PHYSICOCHEMICAL ENGINEERINGS
SCHOOL OF CHEMICAL ENGINEERING
DOCTORATE IN CHEMICAL ENGINEERING
BUCARAMANGA**

2015

ACKNOWLEDGMENTS

I would like to thank Professor Viatcheslav Kafarov for his help with administration during this research.

I must express my sincere appreciation to Professor Maria Paola Maradei García. Without her valuable support, patience, guidance, and encouragement, this research would be impossible to complete. She always took my problems as her own, helped me to overcome them, and encouraged me to achieve the highest level. I will be forever in debt to her.

I am especially indebted to Professor Arnold Rafael Romero Bohorquez for providing me his expertise in the area of purification and characterization of chemical compounds. I was very fortunate to work with him.

My special gratitude also goes to Professor Dennis Wiesenborn for his excellent supervision during my internship at North Dakota State University and his support during my stay in Fargo. His wisdom and commitment to the highest standards motivated me, and his kindness made me to feel at home.

Several people helped me immensely during my entire doctoral program, and I owe my deepest gratitude to them all: Professor Julio Andres Pedraza Avella, Dr. Darrin Haagenson, Dr. Ayhan Dağdelen, Dr. Gülcan Özkan, Nathalia Bedoya Carvajal, Guillermo Acero Medina, Magda Lorena Serrano Barrera, Karoll Yesenia Tiría Peña, and Carlos Andrés Ortiz Bravo.

I gratefully acknowledge the support of the Departamento Administrativo de Ciencia, Tecnología e innovación, COLCIENCIAS, through the Francisco José de Caldas doctoral training program; and the Instituto Colombiano del Petróleo ICP-Ecopetrol. I also gratefully acknowledge Ecodiesel Colombia S.A. for providing the

palm oil biodiesel and precipitate samples for this research, and EP Minerals, LLC and Oil-Dri Corporation of America for providing the adsorbent samples. Sincere appreciation is extended to Maribel Castañeda from the Chromatography Laboratory at ICP-Ecopetrol for her excellent assistance with the GC-FID analyses.

I also wish to thank my examiners for taking time for critically reviewing this thesis.

Last but not least, I would like to extend my special thanks with sincere gratitude to my parents Josué and Blanca Nubia, my brother Josué Mauricio, my sister Diana Marcela, my wife Tatiana, and all close friends and colleagues for their love, prayers, and moral support.

This thesis is dedicated to my beloved wife Tatiana, our children Juan Camilo, Miguel Ángel, Sara Isabel, Esteban, Salomé, and the baby who is on the way

TABLE OF CONTENTS

	Page
INTRODUCTION.....	18
1. BIODIESEL, MINOR COMPONENTS, AND PRECIPITATE FORMATION	20
1.1. OVERVIEW OF BIODIESEL AND MINOR COMPONENTS.....	20
1.2. OVERVIEW OF PRECIPITATE FORMATION	23
1.3. OVERVIEW OF PALM OIL BIODIESEL IN COLOMBIA.....	24
2. FRACTIONATION AND CHARACTERIZATION OF PRECIPITATE ISOLATED FROM PALM OIL BIODIESEL.....	26
2.1. INTRODUCTION	26
2.2. MATERIALS AND METHODS.....	28
2.2.1. Materials	28
2.2.2. Biodiesel analysis.....	29
2.2.3. Sample purification	29
2.2.4. Solubility tests.....	30
2.2.5. Column chromatography.....	30
2.2.6. Characterization	31
2.2.6.1. TLC and FTIR.....	31
2.2.6.2. GC-FID	32
2.2.6.3. DSC and TGA.....	32
2.3. RESULTS AND DISCUSSION.....	33
2.3.1. Biodiesel analysis.....	33
2.3.2. Sample purification	34
2.3.3. Solubility tests.....	35
2.3.4. Column chromatography.....	36
2.3.5. Characterization	36
2.3.5.1. TLC and FTIR.....	36
2.3.5.2. GC-FID	40

2.3.5.3. DSC and TGA.....	42
2.4. CONCLUSIONS	48
3. INFLUENCE OF MINOR COMPONENTS ON PRECIPITATE FORMATION AND FILTERABILITY OF PALM OIL BIODIESEL.....	50
3.1. INTRODUCTION	50
3.2. MATERIALS AND METHODS.....	51
3.2.1. Materials	51
3.2.2. Biodiesel analysis.....	51
3.2.3. Preparation of biodiesel samples.....	51
3.2.4. Cold soak filtration test	52
3.2.5. Experimental design	54
3.3. RESULTS AND DISCUSSION.....	55
3.3.1. Biodiesel analysis.....	55
3.3.2. Model fitting.....	58
3.3.3. Model validation.....	60
3.3.4. Effect of FSG, monoglycerides, and moisture.....	62
3.4. CONCLUSIONS	66
4. IMPROVEMENT OF PALM OIL BIODIESEL FILTERABILITY BY ADSORPTION METHODS.....	68
4.1. INTRODUCTION	68
4.2. MATERIALS AND METHODS.....	69
4.2.1. Materials	69
4.2.2. Sample conditioning	69
4.2.3. Adsorbent treatment	69
4.2.4. Cold soak filtration test	70
4.2.5. Biodiesel analysis.....	71
4.2.6. Steryl glucosides analysis.....	71
4.2.7. Statistical analysis.....	72
4.3. RESULTS AND DISCUSSION.....	73
4.3.1. Adsorbent treatment	75
4.3.1.1. Influence on CSFT.....	75

4.3.1.2. Influence on minor components content and biodiesel properties.....	78
4.3.1.2.1. Total Glycerin	78
4.3.1.2.2. Free sterol glucosides.....	79
4.3.1.2.3. Moisture content	81
4.3.1.2.4. Oxidative stability index	82
4.3.2. Model fitting.....	84
4.3.3. Effect of adsorbent concentration and contact time	86
4.4. CONCLUSIONS	89
5. GENERAL CONCLUSIONS AND RECOMMENDATIONS FOR FUTURE RESEARCH.....	90
REFERENCES	92
SCIENTIFIC NOVELTY	102

LIST OF TABLES

	Page
Table 1. Estimated yields of different biodiesel feedstocks.....	244
Table 2. Biodiesel plants working in Colombia by 2014.....	255
Table 3. Identity of precipitate originated at various locations.....	266
Table 4. Solvent mixtures used for fractionation by column chromatography.	311
Table 5. Fatty acid composition of as-received POB.	333
Table 6. Selected properties for as-received POB, relative to EN limits.	344
Table 7. Mass of fractions extracted from Hz1 and Hz2 by column chromatography.....	366
Table 8. Selected properties for DPOB, as received and spiked with F1Hz1, F2Hz1, and F1Hz2.....	411
Table 9. Representative TGA data of F1Hz1 and the monopalmitin (MP) standard.....	477
Table 10. Representative TGA data of F2Hz1, F1Hz2, and the FSG standard.....	488
Table 11. Amounts of FSG stock solution, monopalmitin and monoolein standards, humidified and dried biodiesel blended to prepare the 300 mL spiked DPOB samples.	533
Table 12 Fatty acid composition of as-received DPOB in comparison with that of typical POB (Prada <i>et al.</i> , 2011).....	566
Table 13. Selected properties for as-received and humidified DPOB.	577
Table 14. Central composite design examining the effect of FSG, monoglycerides (MG), and moisture content on CSFT and the precipitate content of POB.	599
Table 15. Confirmatory experiments to validate the regression model predictions for CSFT and the precipitate content of POB, given FSG, monoglycerides (MG), and moisture content.	611

Table 16. Two central composite designs examining the effect of AABE concentration and contact time on CSFT of POB.844

Table 17. Confirmatory experiments to validate the regression model prediction for CSFT of treated POB, given AABE concentration and contact time. Adsorption temperature: 25°C.866

LIST OF FIGURES

	Page
Figure 1. Transesterification reaction for biodiesel production. R ₁ , R ₂ , and R ₃ denote long-chain saturated or unsaturated hydrocarbons; R ₄ denotes alkyl group (CH ₃ = methanol; C ₂ H ₅ = ethanol).....	21
Figure 2. Structure of β -sitosteryl glucoside. R represents hydrogen in the free form and a long chain fatty acid in the acylated form	22
Figure 3. TLC analysis of F1Hz1, F2Hz1, F1Hz2, and the monopalmitin (MP) and FSG standards. TLC plates were eluted using hexane/ethyl acetate (1/1 v/v) (A) and ethyl acetate/methanol (10/1 v/v) (B) and revealed by exposure to iodine vapor.	37
Figure 4. FTIR spectra of F1Hz1 and the monopalmitin standard (A); F2Hz1, F1Hz2, and the FSG standard (B); and F2Hz1 and the ASG standard (C) in the wavenumber range of 4000-400 cm ⁻¹	37
Figure 5. FTIR spectra of Hz1 and Hz2 in the wavenumber range of 4000-400 cm ⁻¹	40
Figure 6. Representative GC-FID chromatograms of DPOB spiked with F1Hz1 (A), F2Hz1 (B), and F1Hz2 (C). Peaks detected in the range of 17.5-18.5 min corresponded to FSG. Limit of detection: 1.9 mg L ⁻¹	41
Figure 7. Representative GC-FID chromatogram of DPOB spiked with F1Hz1. Peaks detected at 5.5 and 19.2 min corresponded to the internal standards, namely butanetriol and tricaprin, respectively, while in the range of 9-11 min corresponded to fatty acid esters of the POB and in the range of 14.5-16.8 corresponded to monoglycerides. Peaks represented in red corresponded to a standard mixture of monoglycerides.	43
Figure 8. DSC curves of the monopalmitin standard (A) and F1Hz1 (B).....	44
Figure 9. DSC curves of the FSG standard (A), F2Hz1 (B), and F1Hz2 (C).....	46

Figure 10. Representative GC-FID chromatograms of non-spiked DPOB (A) and DPOB spiked with FSG (30 mg L⁻¹) (B). Peaks detected in the range of 17.5-18.5 min corresponded to FSG. Limit of detection: 1.9 mg L⁻¹.....57

Figure 11. Measured precipitate contents versus values predicted by the regression model given in Eq. (5).61

Figure 12. Measured CSFT versus values predicted by the regression model given in Eq. (4).62

Figure 13. Response surface of the combined effect of FSG and moisture on CSFT of POB. The third factor was held at the middle level in generating this plot (monoglycerides, 0.2 mass%).....64

Figure 14. Response surface of the combined effect of FSG and moisture on the precipitate content of POB. The third factor was held at the middle level in generating this plot (monoglycerides, 0.2 mass%).....65

Figure 15. Response surface of the combined effect of monoglycerides (MG) and moisture on the precipitate content of POB. The third factor was held at the middle level in generating this plot (FSG, 20 mg L⁻¹).....66

Figure 16. Cold soak filtration time (A) and precipitate content (B) for treated POB. Control denotes the untreated POB. Treatments having different letters are significantly different by Tukey multiple range test (*p*-value <0.05). The dotted line in A indicates the 360 s ASTM maximum limit for CSFT.....74

Figure 17. Relationship between CSFT and precipitate content of POB subjected to different adsorbent treatments. The dotted line indicates the 360 s ASTM maximum limit for CSFT. Only treatments for which precipitate content was lower than 40 mg L⁻¹ (1 and 5 mass% NS at 25 °C; 5 mass% NBE and AABE at 25 and 110 °C) are represented in this plot, including treatments with NBE (precipitate content = 26.2 mg L⁻¹) and AABE (precipitate content = 14.8 mg L⁻¹) at 40°C. Error bars show standard deviation.....77

Figure 18. Total glycerin content for treated POB. Treatments having different letters are significantly different by Tukey multiple range test (*p*-value <0.05). The

dotted line indicates the 0.24 mass% ASTM maximum limit for total glycerin content.79

Figure 19. Reverse phase HPLC-ELSD chromatogram of centrifuged untreated (A), and centrifuged treated (25 °C and 5 mass% AABE) POB (B). Peaks detected in the range of 5.8-8.2 min corresponded to FSG while in the range of 2.2-3.1 min corresponded to monoglycerides (MG) and in the range of 4.0-5.5 min corresponded to fatty acid esters (FAME) of residual POB. Before analysis, sample A was diluted 1/10 with dichloromethane/methanol (2/1, v/v); sample B, in contrast, was not diluted.80

Figure 20. Moisture content for treated POB. Treatments having different letters are significantly different by Tukey multiple range test (p -value <0.05). The dotted line indicates the 500 mg L⁻¹ EN 14214 maximum limit for moisture content.82

Figure 21. OSI value for treated POB. Treatments having different letters are significantly different by Tukey multiple range test (p -value <0.05). The dotted line indicates the 3 h ASTM minimum limit for OSI value.83

Figure 22. Contour plot for the combined effect of adsorbent concentration and contact time on CSFT for treated POB. The ASTM D6751 Standard Specification stipulates that CSFT should not exceed 360 s. In some instances, a more stringent limit of 200 s is used.87

RESUMEN

TÍTULO: ESTUDIO DE LOS FACTORES DE FORMACIÓN DE PRECIPITADOS EN EL BIODIESEL DE PALMA AFRICANA*

AUTOR: VLADIMIR PLATA CHÁVEZ**

PALABRAS CLAVES: Esteril glucósidos libres, monoglicéridos, filtrabilidad, metodología de superficie de respuesta, tierras de blanqueo

DESCRIPCIÓN:

Este trabajo tuvo como objetivo investigar los factores de formación de precipitados en el biodiesel de palma africana (POB) con el fin de encontrar un set de condiciones donde el POB tuviera un CSFT aceptable. Inicialmente, precipitados aislados de POB fueron fraccionados mediante cromatografía en columna y caracterizados mediante TLC, FTIR, GC-FID, DSC y TGA. La caracterización reveló la presencia preponderante de monopalmitina y esteril glucósidos libres (FSG), sugirió la presencia de esteril glucósidos acilados y jabones de ácidos grasos, y reveló la presencia de componentes desconocidos que pudieron haber eluido con la monopalmitina y los FSG durante el fraccionamiento mediante cromatografía en columna.

Después, se investigó el efecto del contenido de FSG, monoglicéridos y humedad sobre la masa de precipitados y el CSFT del POB.. Se encontró que sólo los FSG afectaban el CSFT mientras que los FSG, monoglicéridos y la humedad afectaban la masa de precipitados. A niveles bajos de humedad, el incremento de FSG incrementó la masa de precipitados. Por el contrario, al incrementarse los monoglicéridos, la masa de precipitados decreció. La interacción con la humedad exacerbó la precipitación.

Finalmente, se investigó el efecto de cuatro adsorbentes sobre el CSFT del POB. Se investigó también el impacto sobre el contenido de glicerina total y de humedad, y la estabilidad oxidativa del biodiesel. Todos los tratamientos disminuyeron la masa de precipitados y el contenido de glicerina total y de humedad, pero sólo el tratamiento con 5 % en peso de un silicato natural y tierras de blanqueo a 25 °C produjo una filtrabilidad aceptable. Las condiciones de adsorción con tierras de blanqueo ácidas (AABE) se optimizaron posteriormente. La combinación de 0.65 % en peso de AABE y 10 min a 25 °C disminuyó el CSFT por debajo del límite de la ASTM.

* Tesis doctoral

** Facultad de Ingenierías Físicoquímicas, Escuela de Ingeniería Química, Director Dr. Sc. Viatcheslav Kafarov, Codirector Ph.D. María Paola Maradei García

ABSTRACT

TITLE: STUDY OF FACTORS AFFECTING PRECIPITATE FORMATION IN PALM OIL BIODIESEL *

AUTHOR: VLADIMIR PLATA CHÁVEZ**

KEY WORDS: Free steryl glucosides, monoglycerides, filterability, response surface methodology, bleaching earths

DESCRIPTION:

This research aimed to investigate the factors affecting precipitate formation in palm oil biodiesel (POB) to find a set of conditions where POB had a passing CSFT. To achieve this goal, precipitates isolated from POB were fractionated by column chromatography and then characterized using TLC, FTIR, GC-FID, DSC, and TGA. Characterization revealed the preponderant presence of monopalmitin and free steryl glucosides (FSG) in the precipitates. FTIR suggested the presence of acylated steryl glucosides and fatty acid soaps, and thermal analysis revealed the presence of unknown components that may have eluted with the monopalmitin and FSG during fractionation by column chromatography.

Subsequently, the effect of FSG, monoglycerides, and moisture content on precipitate formation and filterability of POB was investigated. Blends of distilled palm oil biodiesel spiked with the minor components were prepared and tested for CSFT and the precipitate content. CSFT was found to be influenced only by FSG whereas the precipitate content was found to be influenced by FSG, monoglycerides, and moisture. Increasing FSG increased precipitation at low levels of moisture; in contrast, when monoglycerides increased, the precipitate content decreased. Interaction with moisture exacerbated precipitation.

Lastly, the effect of four adsorbents on the precipitate content and CSFT of POB was investigated. The impact on total glycerin content, moisture content, and oxidative stability was also examined. All treatments significantly decreased the precipitate content, total glycerin content, and moisture content, but only treatments with natural silicate and bleaching earths at 5 mass% and 25 °C achieved acceptable filterability. The OSI value was also decreased; however, it remained above the ASTM limit. Operational conditions of treatment with acid activated bleaching earth (AABE) were further optimized in a two-factor, five-level center composite design. The combination of 0.65 mass% AABE and 10 min at 25°C decreased CSFT to below the ASTM limit.

* Doctoral thesis

** Faculty of Physicochemical Engineerings, School of Chemical Engineering, Supervisor Dr. Sc. Viatcheslav Kafarov, Supervisor Ph.D. María Paola Maradei García

INTRODUCTION

In Colombia, palm is the most important oleo-chemical feedstock, and 9 biodiesel plants are currently working. These plants are the centerpiece of the Colombian Biofuel National Program. However, palm oil biodiesel (POB) is characterized by a very precipitate content and high cold soak filtration time (CSFT). Precipitate induces a number of undesired consequences, which causes potential customers to view biodiesel unfavorably and places the acceptability of this biofuel at risk. Therefore, this research aimed to investigate the factors affecting precipitate formation in POB to find a set of conditions where POB had a passing CSFT through fractionation and characterization of precipitates isolated from POB; investigating the effect of minor components on precipitate formation and filterability of POB; and improving POB filterability through selection of an adsorbent capable of substantially decreasing the precipitate content.

To achieve this goal, precipitates isolated from POB were fractionated by column chromatography and then characterized using thin layer chromatography, FTIR, GC-FID, differential scanning calorimetry, and thermogravimetric analysis. Characterization revealed the preponderant presence of monopalmitin and free steryl glucosides (FSG) in the precipitates. FTIR suggested the presence of acylated steryl glucosides and fatty acid soaps, and thermal analysis revealed the presence of unknown components that may have eluted with the monopalmitin and FSG during fractionation by column chromatography. All these findings resulted in the development of a technique to improve POB filterability not only focused on the removal of FSG from POB.

Subsequently, the effect of FSG, monoglycerides, and moisture content on precipitate formation and filterability of POB was investigated. Blends of distilled palm oil biodiesel spiked with the minor components were prepared following a three-factor, five-level center composite design and tested for CSFT (ASTM

D7501) and the precipitate content (ASTM D7321). CSFT was found to be influenced only by FSG whereas the precipitate content was found to be influenced by FSG, monoglycerides, and moisture. Increasing FSG increased precipitation at low levels of moisture; in contrast, when monoglycerides increased, the precipitate content decreased. Interaction with moisture exacerbated precipitation. A model capable of explaining 80% of the CSFT variability and a model capable of explaining more than 96% of the precipitate content variability were obtained using multiple regression analysis.

Lastly, the effect of four adsorbents, namely diatomaceous earth, natural silicate (NS), neutral bleaching earth (NBE), and acid activated bleaching earth (AABE), at two levels of addition (1 and 5 mass%) or two temperatures (25 and 110 °C), on the precipitate content and CSFT of POB was investigated. The impact on total glycerin content, moisture content, and oxidative stability was also examined. All treatments significantly decreased the precipitate content, total glycerin content, and moisture content, but only treatments with NS, NBE, and AABE at 5 mass% and 25 °C achieved acceptable filterability. The OSI value was also decreased; however, it remained above the ASTM limit. Operational conditions of treatment with AABE were further optimized in a two-factor, five-level center composite design. The combination of 0.65 mass% AABE and 10 min at 25°C decreased CSFT to below the ASTM limit. Lower adsorbent concentrations could be effective down to 0.44 mass%, given a corresponding increase in the contact time up to 30 min.

1. BIODIESEL, MINOR COMPONENTS, AND PRECIPITATE FORMATION¹

1.1. OVERVIEW OF BIODIESEL AND MINOR COMPONENTS

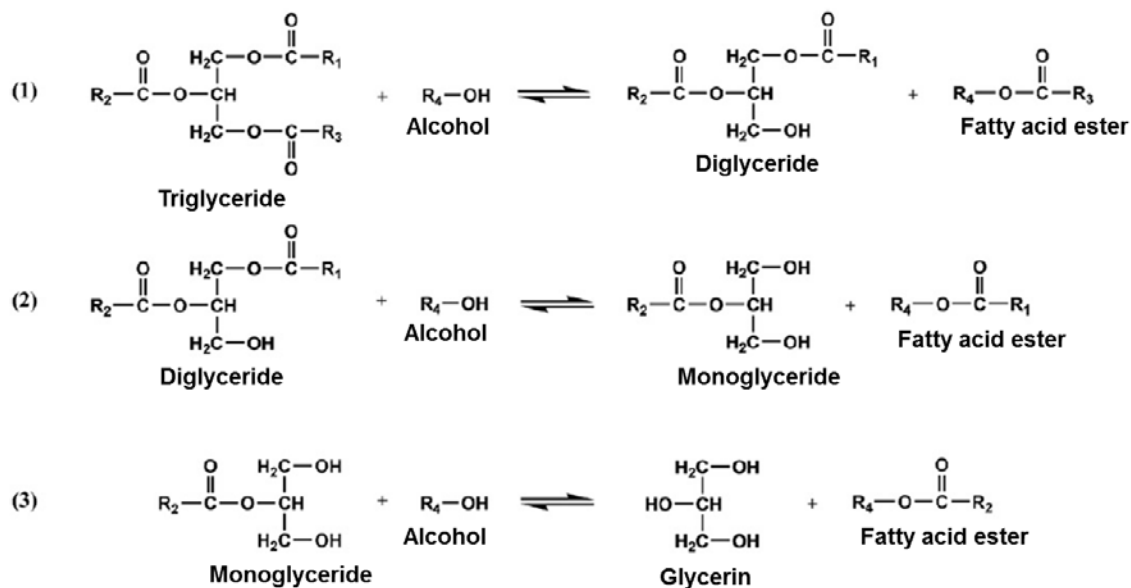
Diesel fuels from petroleum have long played an important role in industry and transportation. However, alternative fuels have become important worldwide during the last two decades. One of these alternatives is biodiesel, which is composed of mono-alkyl esters of long chain fatty acids derived from vegetable oils or animal fats (Knothe *et al.*, 2005). Interest in biodiesel has been primarily motivated by concerns about greenhouse gas emissions and global climate change, a desire for renewable/sustainable energy sources, and an interest in developing domestic and more secure fuel supplies (Hoekman *et al.*, 2012). Biodiesel offers the advantage that it is renewable, biodegradable and non-toxic; it also reduces greenhouse gas emissions (Knothe *et al.*, 2005). It can be used, directly or blended with diesel fuel, to run existing diesel engines without major modifications of the engines and with the same or better performance in comparison to ordinary diesel fuel (Mekhilef *et al.*, 2011); when blended with diesel fuel, biodiesel improves lubricity (Knothe *et al.*, 2005).

Biodiesel is commonly produced via transesterification of oils or fats. Transesterification has been described as the chemical reaction between triglycerides in the oils or fats and a short chain, monohydric alcohol in the presence of a catalyst (Sharma and Singh, 2009). The process generally follows three steps. As depicted in Fig. 1, reaction (1) converts a triglyceride into a diglyceride and a fatty acid ester. Subsequently, reaction (2) produces a monoglyceride and another fatty acid ester. Lastly, reaction (3) produces glycerin

¹ This chapter is based on the paper "*Improving the low-temperature properties and filterability of biodiesel*" by Vladimir Plata, Viatcheslav Kafarov, and Edgar Castillo, published in *Chemical Engineering Transactions* (2012) 29:1243-1248
<http://dx.doi.org/10.3303/CET1229208>

and a third fatty acid ester. Thus, at complete conversion, one mole of triglyceride will produce three moles of fatty acid ester (Dunn, 2009).

Figure 1. Transesterification reaction for biodiesel production. R_1 , R_2 , and R_3 denote long-chain saturated or unsaturated hydrocarbons; R_4 denotes alkyl group (CH_3 = methanol; C_2H_5 = ethanol).



Source: Dunn, 2009

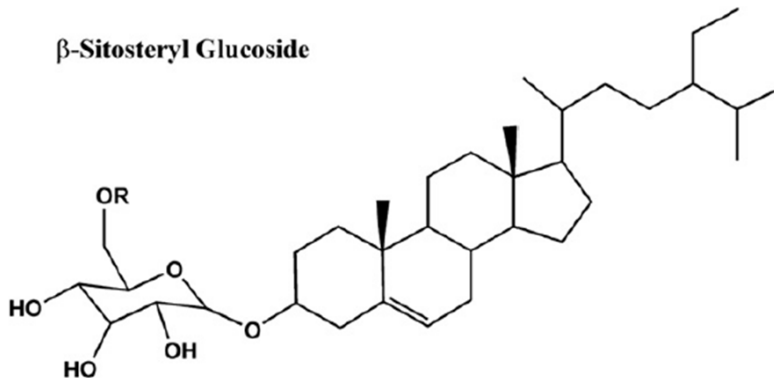
The crude product of transesterification consists mainly of fatty acid esters (≥ 96.5 mass%) and minor components such as diglycerides, monoglycerides, glycerin, catalyst, and fatty acid soaps² present at trace levels (Atadashi *et al.*, 2010). These minor components are referred to as contaminants. Residual glycerin, catalyst, and fatty acid soaps are typically removed during biodiesel refining by washing with acidified water (Van Gerpen, 2005); however, traces thereof can be found in the final biodiesel (Knothe, 2006). Residual diglycerides and monoglycerides are not soluble in water and may remain in the final biodiesel. Other minor components

² Alkali-catalyzed transesterification of feedstock oils containing significant amounts of free fatty acids (≥ 0.5 mass%) leads to formation of fatty acid soaps (Sharma and Singh, 2009)

following the process include antioxidants and sterols, which are naturally present in vegetable oils (Dunn, 2009).

Steryl glucosides are another type of biodiesel minor component. They are glycosylated sterol derivatives naturally present in vegetable oils and occur in both free sterol glucosides (FSG) and acylated sterol glucosides (ASG) form (Tang *et al.*, 2010). In ASG, the 6-position of the glucose is esterified with a long chain fatty acid (Fig. 2). Under alkaline conditions, the ester bond between the glucose and the fatty acid is broken, and an ASG is converted into its free form. Such a side reaction occurs during transesterification, resulting in an increased FSG content in biodiesel in comparison with the initial amount in the feedstock oil (Van Hoed *et al.*, 2008).

Figure 2. Structure of β -sitosteryl glucoside. R represents hydrogen in the free form and a long chain fatty acid in the acylated form



Source: Dunn, 2009

FSG content of biodiesel may vary markedly depending on the feedstock oil, the oil refining processes and the biodiesel production processes (Tang *et al.*, 2010). It may range from not detectable to 158 ppm for soybean oil biodiesel, and from 55 to 275 ppm for palm oil biodiesel (POB) (Van Hoed *et al.*, 2008). FSG has limited solubility in biodiesel (56 mg L⁻¹ at 20 °C in POB, Lacoste *et al.*, 2009) and may act

as nucleators for biodiesel precipitate formation. FSG may form complexes with residual diglycerides and monoglycerides, and complexes may interact with moisture, exacerbating precipitate formation (Dunn, 2009).

1.2. OVERVIEW OF PRECIPITATE FORMATION

Precipitate formation is a big concern for biodiesel producers. At the beginning, a cloud of tiny precipitate is dispersed through the entire volume of the biodiesel, thereby causing a loss of transparency and brilliancy. In some instances, precipitation manifests itself within a short time after biodiesel production and at temperatures above the cloud point (Van Hoed *et al.*, 2008). The cloud point is the temperature when the smallest observable cluster of fatty acid ester crystals first occurs upon cooling under prescribed conditions (ASTM D2500).

Precipitate induces a number of undesired consequences: it may affect process equipment upstream of the tank farm in biodiesel facilities; it may also settle at the bottom of biodiesel storage tanks. As a consequence, frequent maintenance is necessary in biodiesel facilities (Van Hoed *et al.*, 2008). More important, precipitate has also caused clogging of fuel filters in engine fuel delivery systems and engine failure due to fuel filter clogging (Kotrba, 2006), thereby causing potential customers to view biodiesel unfavorably.

In an effort to address the fuel filter clogging potential of biodiesel, the American Society for Testing and Materials (ASTM) developed a cold soak filtration test, which was included in the ASTM D6751 Standard Specification as cold soak filterability (ASTM D6751). This test, denominated as the ASTM D7501 Standard Test Method (ASTM D7501), was intended to determine if biodiesel is sufficiently free of precipitate capable of clogging fuel filters. The cold soak filtration test consists of chilling the biodiesel for a specified time and then allowing it to warm to ambient temperature prior to filtration through a specific filtration apparatus and

under prescribed conditions. The ASTM D6751 Standard Specification requires that biodiesel have a cold soak filtration time (CSFT) below 360 s.

1.3. OVERVIEW OF PALM OIL BIODIESEL IN COLOMBIA

Palm oil has several outstanding characteristics as a feedstock for biodiesel production. Palm is a perennial crop, unlike soybean and rapeseed (Mekhilef *et al.*, 2011). Perennial crop means that the production of oil is continuous and uninterrupted (Lam *et al.*, 2009). Palm plantations have the highest oil yield in terms of oil production per hectare per year (Table 1) (Atabani *et al.*, 2010). Oil yield from palm (5950 L) is more than five-fold higher than oil yields from soybean (446 L) and rapeseed (1190 L), which are preferably used for biodiesel production in USA and Europe, respectively (Sharma and Singh, 2009). In Colombia, palm is the most important oleo-chemical feedstock, and 9 biodiesel plants with an annual capacity of 581,000 tonnes are currently working (Table 2), making Colombia one of the leaders of biodiesel production in Latin America (Janssen and Rutz, 2011). These plants are the centerpiece of the Colombian Biofuel National Program, which was designed to develop the agricultural sector, generate permanent jobs, improve the air quality, and replace illicit crops (Fedepalma, 2014a).

Table 1. Estimated yields of different biodiesel feedstocks.

Feedstock	Oil yield (liter per hectare per year)
Castor	1413
Cottonseed	325
Jatropha	1892
Karanja	225
Palm	5950
Soybean	446
Sunflower	952
Rapeseed	1190

Source: Atanabi *et al.*, 2012

Several policies were established to implement, regulate, and support the production, transit and use of biodiesel in Colombia. The Law 693 of 2001 and the Law 939 of 2004 were the basis for technical policies, tax exemptions, and quality standards; and a mandatory blend of diesel and biodiesel has been gradually implemented throughout the Colombian territory in accordance with the Decree 2629 of 2007 (Rincón *et al.*, 2015). The existing biodiesel blends are B2 (2 mass% biodiesel in diesel) in the eastern zone, B8 in the middle zone, and B10 in the northern, western, and southern zones (Fedepalma, 2014a); and it is expected that biodiesel demand will expand to B20 blend by 2020 (Rincón *et al.*, 2015). However, POB is characterized by very poor filterability, resulting in failing CSFT (Tang *et al.*, 2008a). Thus, Biofuel National program will be put at risk if POB filterability is not improved. Therefore, based on the hypothesis that it is possible to find a set of conditions where POB had a passing CSFT through investigating the factors affecting precipitate formation in biodiesel, this research aimed to investigate the factors affecting precipitate formation in POB.

Table 2. Biodiesel plants working in Colombia by 2014.

Region, City	Company	Capacity (tonne per year)
Northern, Codazzi	Oleoflores	60,000
Middle, Barrancabermeja	Ecodiesel Colombia	115,000
Eastern, Facatativá	BioD	115,000
Northern, Santa Marta	Biocombustibles Sostenibles del Caribe	100,000
Eastern, San Carlos de Guaroa	Aceites Manuelita	120,000
Northern, Barranquilla	Romil de la Costa	10,000
Northern, Gálapa	Biodiesel de la Costa	10,000
Northern, Santa Marta	Odín Energy	36,000
Eastern, Castilla la Grande	Biocastilla	15,000

Source: Fedepalma, 2014a

2. FRACTIONATION AND CHARACTERIZATION OF PRECIPITATE ISOLATED FROM PALM OIL BIODIESEL³

2.1. INTRODUCTION

Most techniques developed so far to prevent biodiesel precipitate formation have focused on either the removal of FSG present in biodiesel by physical means such as adsorption (Sohling *et al.*, 2011) or the chemical modification of FSG by enzymatic acylation or hydrolysis present in biodiesel (Brask and Nielsen, 2012; Aguirre *et al.*, 2014). FSG are glycosylated steryl derivatives naturally present in vegetable oils (Lacoste *et al.*, 2009). Because of their limited solubility in biodiesel, researchers have reported that FSG are the main cause of precipitate formation (Van Hoed *et al.*, 2008; Lacoste *et al.*, 2009; Bondioli *et al.*, 2008). However, trace contaminants different from FSG have been identified in biodiesel precipitate (Table 3).

Table 3. Identity of precipitate originated at various locations.

Feedstock oil	Origin	Analysis	Precipitate identity	Ref.
Soybean Palm	Turbid biodiesel, solid material: polish filter cake	GC-FID, NMR	FSG FSG	Van Hoed <i>et al.</i> , 2008
Soybean Palm	Solid material: washing centrifuge residue	FTIR, GC-FID	FSG FSG	Bondioli <i>et al.</i> , 2008
Soybean Cotton seed	Turbid biodiesel	FTIR, GC-FID	FSG FSG, monoglycerides, free and acylated sterols Monoglycerides	Tang <i>et al.</i> , 2008b
Poultry fat				

³ This chapter is based on the paper “*Characterization of insoluble material isolated from Colombian palm oil biodiesel*” by Vladimir Plata, Paola Gauthier-Maradei, Arnold R. Romero-Bohórquez, Viatcheslav Kafarov, and Edgar Castillo, published in *Biomass and Bioenergy* (2015) 74:6-14
<http://dx.doi.org/10.1016/j.biombioe.2014.12.024>

Table 3. (Continuation)

Feedstock oil	Origin	Analysis	Precipitate identity	Ref.
Soybean	Turbid biodiesel, solid or semisolid material: polish filter cake, transit pipe residue, storage tank bottoms	HPLC-ELSD, HPLC-MS	FSG	Moreau <i>et al.</i> , 2008
Soybean Palm	Turbid biodiesel	FTIR, GC-FID	FSG Monoglycerides	Tang <i>et al.</i> , 2008a
Soybean Palm	Turbid biodiesel, solid material: washing centrifuge residue	FTIR, TLC, GC-FID	Saturated monoglycerides FSG	Bondioli, 2009
Soybean	Turbid biodiesel	FTIR	FSG	Wang <i>et al.</i> , 2010
Soybean	Turbid biodiesel/ultra low sulfur diesel B20 blend	GC-FID, GC-MS	FSG, monoglycerides, unsaturated esters oxidation byproducts	McGinnis and Peyton, 2010
Canola	Semisolid material: storage tank bottoms	FTIR	Fatty acid soaps, glycerin	Lin <i>et al.</i> , 2011
Soybean	Solid material: fuel filter deposits	FTIR, GC-MS	FSG, unsaturated esters oxidation byproducts	Lopez <i>et al.</i> , 2011
Canola	Turbid biodiesel	MALDI-TOF MS	Sterols, monoglycerides, saturated diglycerides	McAlpin <i>et al.</i> , 2011
Beef tallow Yellow grease Canola	Turbid biodiesel	NMR	Saturated glycerides	Farahani <i>et al.</i> , 2011
Beef tallow	Turbid biodiesel	GC-FID, TGA	Saturated monoglycerides	Fernandes Júnior <i>et al.</i> , 2012

Most of papers regarding the isolation, purification, and characterization of biodiesel precipitate published so far have focused on soybean oil biodiesel (Table 3), and papers focused on POB have been contradictory. Van Hoed *et al.* (2008) found that FSG were the major constituent of the cake collected after filtration of biodiesel between storage tanks in a POB facility. Analogous results were reported by Bondioli *et al.* (2008) and Bondioli (2009) for the solid material isolated from a centrifuge in the water washing stage of a POB facility. In contrast, Tang *et al.* (2008a) identified only monoglycerides in the precipitate isolated from turbid POB. Therefore, the objective of this chapter was to characterize precipitates isolated from POB. The precipitates were purified by successive washes with hexane, then fractionated by column chromatography, and then characterized using thin layer chromatography (TLC), FTIR, GC-FID, differential scanning calorimetry (DSC), and thermogravimetric analysis (TGA).

2.2. MATERIALS AND METHODS

2.2.1. Materials

POB was supplied by Ecodiesel Colombia S.A. (Barrancabermeja, Colombia). Distilled palm oil biodiesel (DPOB) was provided by the Colombian Petroleum Institute (ICP-Ecopetrol, Piedecuesta, Colombia). The POB was prepared from degummed, bleached, and deodorized palm oil and was obtained dynamically from a sampling loop in a distribution line in the processing facility. The DPOB was produced in accordance with the ASTM D5236 Standard Test Method. Two types of precipitate were characterized in this study. The first was collected from the bottom of glass containers in which POB was stored at 20 °C for 1 month; the second was collected from the bottom of storage tanks in which POB was stored at ambient temperature (35-40 °C) for 6 months. All solvents were Carlo Erba Reagents (Milan, Italy) and Honeywell International Inc. (Morris Township, NJ) ACS reagent grade. A monopalmitin standard was obtained from Sigma Aldrich Co. LLC. (St. Louis, MO) and was reported to be >99% pure. FSG and acylated

steryl glucosides (ASG) standard mixtures were obtained from Matreya, Inc. (Pleasant Gap, PA) and were reported to be >98% pure. The composition of the standard mixtures was 56, 25, and 18%, β sitosteryl, campesteryl, and stigmasteryl glucoside, respectively.

2.2.2. Biodiesel analysis

Fatty acid composition of the as-received POB was determined by the Chromatography and Mass Spectrometry Laboratory (CROM-MASS) at the Industrial University of Santander (Bucaramanga, Colombia) in accordance with the ISO 5508:1990 and 5509:2000 Standards. Free and total glycerin content (mass fraction) of the POB was provided by Ecodiesel Colombia S.A. FSG content was determined by the Chromatography Laboratory at ICP-Ecopetrol using a GC-FID method (ICP CLR-CRO-I-091 procedure) developed, validated, and commercialized by them. Details about the ICP CLR-CRO-I-091 procedure are confidential. These analyses were done by the Chromatography Laboratory at ICP-Ecopetrol, which is accredited by the Colombian National Accreditation Agency (ONAC) and the Colombian Hydrology, Metrology, and Environmental Studies Institute (IDEAM). Total contamination was determined by the Crude Evaluation Laboratory at ICP-Ecopetrol in accordance with the European Standard EN 12662.

2.2.3. Sample purification

1 g of precipitate was transferred to a 15 mL centrifuge tube, and 10 mL of hexane were added to the tube. The resulting mixture was centrifuged at 2100 rpm and 20 °C for 15 min using a Hettich Universal 320R centrifuge, and the supernatant was discarded. The pellet was washed two more times, and then dried in an oven at 70 °C for 30 min. The pellet isolated from the precipitate collected from the bottom of the glass containers was denominated as Hz1, and the pellet isolated from the precipitate collected from the bottom of the storage tanks was denominated as Hz2.

2.2.4. Solubility tests

Four solubility tests were done to find a solvent capable of dissolving the pellets for fractionation by column chromatography. This was a critical task because of the limited solubility of biodiesel precipitate in most organic solvents (Lacoste *et al.*, 2009). Precipitate is soluble in pyridine, dimethylsulfoxide (Van Hoed *et al.*, 2008), dimethylacetamide, and methylpyrrolidone (Lacoste *et al.*, 2009), which have high boiling point and are inappropriate to be used in fractionation by column chromatography.

1 mg of pellet was tried to be dissolved in 1 mL of solvent. Dichloromethane, ethyl acetate, methanol/acetone/toluene (1/1/1 v/v/v), and chloroform/methanol (85/15 v/v) were used as solvent. Solubility was measured in terms of nephelometric turbidity units (NTU) by a HACH 2100Q turbidimeter calibrated with certified standard solutions in the range of 0-800 NTU.

2.2.5. Column chromatography

Fractionation by column chromatography was done using a 70 x 30 cm glass column packed with 50 g of silica gel 60 (0.063-0.200 mm, Merck ref no. 1.07734.1000) activated in an oven at 110 °C overnight. The column was packed using the wet slurry method. The silica was slurried in 200 mL of hexane/ethyl acetate (5/1 v/v) for fractionation of Hz1 and in 200 mL of hexane/ethyl acetate (1/10 v/v) for fractionation of Hz2, and the resulting mixture was quickly transferred to the column before the silica settled. A substantial amount of the same solvent mixture was then poured continuously into the column and allowed to drain off but prevented from reaching the top of the silica. 1 g of pellet was dissolved in chloroform/methanol (85/15 v/v), and a small quantity of silica was added to the solution. The resulting mixture was then rotoevaporated at 40 °C and 70 mbar using a Büchi Rotavapor R-200 rotary evaporator to obtain a free flowing powder, and the powdered solid was applied on the top of the column. Additional silica was added to a height of 5 mm. The column was then eluted successively with solvent

mixtures of increasing polarity (Table 4), and the eluate was collected continuously in test tubes. Fractionation was monitored by applying the eluate on TLC silica gel 60 F254 plates (Merck ref. no. 1.05715.0001), eluting the plates with either hexane/ethyl acetate (1/1 v/v) or ethyl acetate/methanol (10/1 v/v), and revealing the plates by exposure to iodine vapor. Test tubes having similar retention factor were combined together, and then evaporated until dryness.

Table 4. Solvent mixtures used for fractionation by column chromatography.

Pellet	Solvent mixture^a	V (mL)	Pellet	Solvent mixture	V (mL)
Hz1	H/EA 5/1 v/v	100	Hz2	H/EA 1/10 v/v	200
	H/EA 2/1 v/v	100		EA	200
	H/EA 1/1 v/v	300		EA/M 10/1 v/v	300
	H/EA 1/2 v/v	200		EA/M 5/1 v/v	300
	H/EA 1/10 v/v	200		EA/M 1/1 v/v	300
	EA	200		M	300
	EA/M 10/1 v/v	300			
	EA/M 5/1 v/v	300			
	EA/M 1/1 v/v	300			
	M	300			

^aH, EA, and M denote hexane, ethyl acetate and methanol, respectively

2.2.6. Characterization

2.2.6.1. TLC and FTIR

The fractions extracted from Hz1 and Hz2 and the monopalmitin and FSG standards were dissolved in chloroform/methanol (85/15 v/v), and then applied on 4 x 4 cm TLC silica gel 60 F254 plates (Merck ref. no. 1.05715.0001). The plates were eluted using either hexane/ethyl acetate (1/1 v/v) or ethyl acetate/methanol (10/1 v/v), and then revealed by exposure to iodine vapor. Retention factor of the fractions was compared with that of the standards.

FTIR spectra were obtained using a Bruker Tensor 27 spectrometer equipped with an attenuated total reflectance (ATR) sampling accessory (with diamond crystal). All spectra were obtained in the wavenumber range of 4000-400 cm⁻¹ using an

average of 16 scans, with a spectral resolution of 4 cm^{-1} , and air as the background.

2.2.6.2. GC-FID

DPOB spiked with the fractions extracted from Hz1 and Hz2 was analyzed for free and total glycerin content and FSG content. About 5 mg of the fractions were dissolved in chloroform/methanol (85/15 v/v), and then added to 25 mL of DPOB via pipette. The resulting mixture was rotoevaporated at $65\text{ }^{\circ}\text{C}$ and 70 mbar for 2 h to evaporate the chloroform/methanol introduced by the stock solution, and then analyzed by the Chromatography Laboratory at ICP-Ecopetrol in accordance with the ASTM D6584 Standard Test Method and the ICP CLR-CRO-I-091 procedure.

2.2.6.3. DSC and TGA

DSC curves of the fractions extracted from Hz1 and Hz2 and the monopalmitin FSG, and ASG standards were obtained using a TA instrument model DSC Q10. Nitrogen as purge gas was passed through the measurement cell at 50 mL min^{-1} . Pure indium supplied by the manufacturer was employed for temperature calibrations. Each sample (~5 mg) was sealed in aluminum Tzero pans, and an empty pan was used as reference. The monopalmitin standard was equilibrated at $20\text{ }^{\circ}\text{C}$ for 1 min, and then heated at $5\text{ }^{\circ}\text{C min}^{-1}$ to $110\text{ }^{\circ}\text{C}$. After remaining at this temperature for 1 min, it was cooled to $0\text{ }^{\circ}\text{C}$ at the same rate, then held isothermally for 1 min, and then reheated to $110\text{ }^{\circ}\text{C}$ at the same rate. The same heat/cool/reheat cycle was applied to one of the fractions extracted from Hz1. The FSG standard was equilibrated at $0\text{ }^{\circ}\text{C}$ for 1 min, and then heated at $5\text{ }^{\circ}\text{C min}^{-1}$ to $350\text{ }^{\circ}\text{C}$. After remaining at this temperature for 1 min, it was cooled to $0\text{ }^{\circ}\text{C}$ at the same rate, then held isothermally for 1 min, and then reheated to $350\text{ }^{\circ}\text{C}$ at the same rate. The same heat/cool/reheat cycle was applied to the ASG standard, the other fraction extracted from Hz1, and the fraction extracted from Hz2.

TGA experiments were conducted using a TA instrument model TGA Q2050 under nitrogen atmosphere at a heating rate of 5 °C min⁻¹ and a gas flow of 50 mL min⁻¹. Each sample had a mass of about 5 mg and was heated from 25 to 750 °C.

2.3. RESULTS AND DISCUSSION

2.3.1. Biodiesel analysis

Methyl palmitate (C16:0) and methyl oleate (C18:1) were the primary fatty acid esters of the as-received POB (Table 5), along with methyl linoleate (C18:2) and methyl stearate (C18:0). Although oxidative stability was not determined in this study, the POB was expected to have high oxidative stability because of its high percentage of saturates, much higher than in other typical biodiesel feedstocks (Tang *et al.*, 2008b). Biodiesel is susceptible to oxidation with a high percentage of unsaturated fatty acids esters, especially methyl linolenate (C18:3) (McCormick *et al.*, 2007), which was present in the POB at trace levels. In addition, POB has natural antioxidants that impart high oxidative stability to biodiesel (Fröhlich and Schober, 2007).

Table 5. Fatty acid composition of as-received POB.

Fatty acid	Mass fraction (%)
C12:0	0.3
C14:0	1.0
C16:0	44.8
C16:1	0.2
C18:0	4.3
C18:1	39.9
C18:2	8.7
C18:3	0.2
C20:0	0.4
C22:0	0.1
C24:0	0.1

Free glycerin and glyceride species (mono-, di-, and tri-) met the European Standard EN 14214 (Table 6); of these minor components, monoglycerides were

the most abundant compared with di- and triglycerides. Since the POB had a high percentage of saturated fatty acids esters (Table 5), monoglycerides were expected to have a similar, high percentage of saturates. When compared to unsaturated monoglycerides, saturated monoglycerides have been demonstrated to favor precipitate formation (Lin *et al.*, 2011). FSG content was almost two-fold higher than FSG solubility in POB at 20°C (56.0 mg L⁻¹, Lacoste *et al.*, 2009). Thus, total contamination was well above the 24 mg L⁻¹ specified in the European Standard EN 14214.

Table 6. Selected properties for as-received POB, relative to EN limits.

Property	EN limit	Unit	POB
MG ^a content	0.80	mass%	0.307
DG content	0.20	mass%	0.190
TG content	0.20	mass%	0.086
Free glycerin content	0.02	mass%	0.010
Total glycerin content	0.24	mass%	0.127
FSG content	N.S. ^b	mg L ⁻¹	110.9
Total contamination	24	mg L ⁻¹	101.9

^aMG, DG, and TG denote mono-, di-, and triglycerides, respectively

^bNot specified

2.3.2. Sample purification

H_z1 and H_z2 were different in appearance and consistency. H_z1 was bright white in color and had a soft consistency whereas H_z2 was brown in color and had a sticky consistency. These differences evidenced significant differences in the constitution of the precipitates. This was consistent with the finding of Moreau *et al.* (2008), who characterized precipitates originated at various locations in the soybean biodiesel supply chain. The authors found that constitution of the precipitates was quite heterogeneous, so that FSG content ranged between 0 and 68 mass%, monoglycerides content ranged between 0 and 7.4 mass%, diglycerides content ranged between 0 and 2.8 mass%, and triglycerides content ranged between 0 and 0.3 mass%.

Storage conditions may significantly impact the constitution of biodiesel precipitate (McGinnis and Peyton, 2010). When exposed to air at temperatures above 40 °C, biodiesel becomes more susceptible to oxidation. At these conditions, a wide variety of polar oxygenated compounds, namely mono-, di-, and hydroxycarboxylic acids; aldehydes, ketones, and their ester derivatives; may arise due to oxidative cleavage of the unsaturated fatty acid esters of the biodiesel, especially methyl linolenate. These polar oxygenated compounds may undergo aggregation because of their polarity differences with the biodiesel and come out of solution to form complexes with residual FSG, glycerides, and other trace contaminants. As a consequence, biodiesel precipitate may contain large amounts of the aforementioned polar oxygenated compounds (McGinnis and Peyton, 2010). However, POB has been demonstrated to be less affected by oxidative degradation than other biodiesel feedstock (Liang *et al.*, 2006), even under long storage times (Moser, 2011). Therefore, Hz2 was not expected to contain the aforementioned polar oxygenated compounds in significant amounts, and the differences between Hz1 and Hz2 was attributed to the presence at different concentrations of trace contaminants inherent to biodiesel, especially saturated monoglycerides, FSG, and fatty acid soaps (Dunn, 2009).

2.3.3. Solubility tests

Hz1 completely dissolved in dichloromethane (NTU <2). In contrast, Hz2 did not dissolve in dichloromethane, ethyl acetate, or methanol/acetone/toluene (1/1/1 v/v/v) (NTU >130). Hz2 partially dissolved in chloroform/methanol (85/15 v/v) (~60 NTU). Therefore, 0.75, 0.50 and 0.25 mg of Hz2 was tried to be dissolved in 1 mL of chloroform/methanol (85/15 v/v). Turbidity fell below 10 NTU at 250 mg L⁻¹. In addition, Hz1 completely dissolved in chloroform/methanol (85/15 v/v), even at 1000 mg L⁻¹. Thus, chloroform/methanol (85/15 v/v) was used to dissolve Hz1 and Hz2 for fractionation by column chromatography.

2.3.4. Column chromatography

Two fractions were extracted from Hz1, namely F1Hz1 and F2Hz1, and one fraction was extracted from Hz2, namely F1Hz2 (Table 7). The mass of F1Hz1 and F1Hz2 was about three-fourths that of Hz1 and Hz2, respectively. Since F1Hz1 and F1Hz2 were extracted using different solvent mixtures, the differences between Hz1 and Hz2 were mainly attributed to the presence of those primary fractions. Therefore, effort was concentrated on characterizing F1Hz1 and F1Hz2.

Table 7. Mass of fractions extracted from Hz1 and Hz2 by column chromatography.

Pellet	Fraction	Mass^a (g)
Hz1	F1Hz1	0.7568 ± 0.0757
	F2Hz1	0.1225 ± 0.0228
Hz2	F1Hz2	0.7374 ± 0.0374

^aMean values ± standard deviation

2.3.5. Characterization

2.3.5.1. TLC and FTIR

When hexane/ethyl acetate (1/1 v/v) was used as eluent (Fig. 3A), F1Hz1 and the monopalmitin standard marked a clear and distinct spot at a retention factor of 0.29. In contrast, F1Hz2, F2Hz1, and the FSG standard did not travel from the origin with the eluent. This suggested that F1Hz1 was composed of monopalmitin. This finding was consistent with FTIR analysis, where a doublet of –OH stretching peak (3299 cm⁻¹), sharp –CH₂ asymmetric and symmetric stretching peaks (2915 and 2850 cm⁻¹), and strong peaks due to –C=O stretching (1730 cm⁻¹) and –CH₂ rocking bending (719 cm⁻¹) were observed in the spectra of F1Hz1 and the monopalmitin standard (Fig. 4A). A series of strong peaks attributable to twisting and wagging bending of –CH₂ was also observed in the region referred as the “finger-print” (1300-900 cm⁻¹). All these signals are characteristic of monoglycerides (Tang *et al.*, 2008a).

Figure 3. TLC analysis of F1Hz1, F2Hz1, F1Hz2, and the monopalmitin (MP) and FSG standards. TLC plates were eluted using hexane/ethyl acetate (1/1 v/v) (A) and ethyl acetate/methanol (10/1 v/v) (B) and revealed by exposure to iodine vapor.

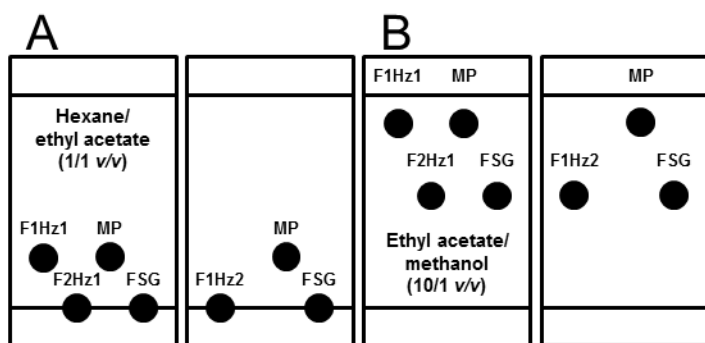


Figure 4. FTIR spectra of F1Hz1 and the monopalmitin standard (A); F2Hz1, F1Hz2, and the FSG standard (B); and F2Hz1 and the ASG standard (C) in the wavenumber range of 4000-400 cm^{-1} .

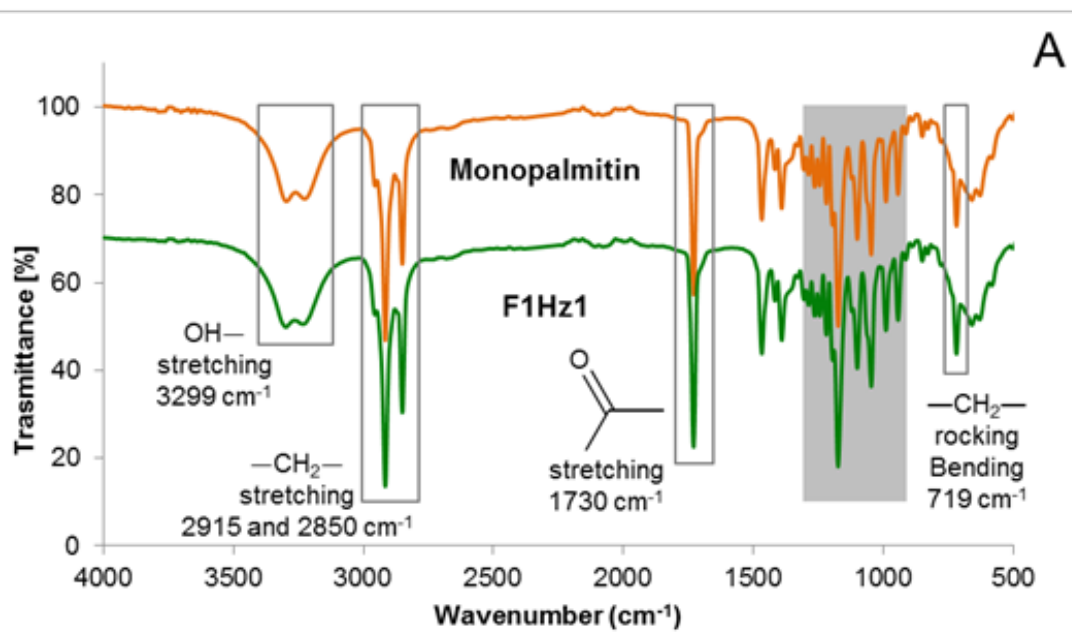
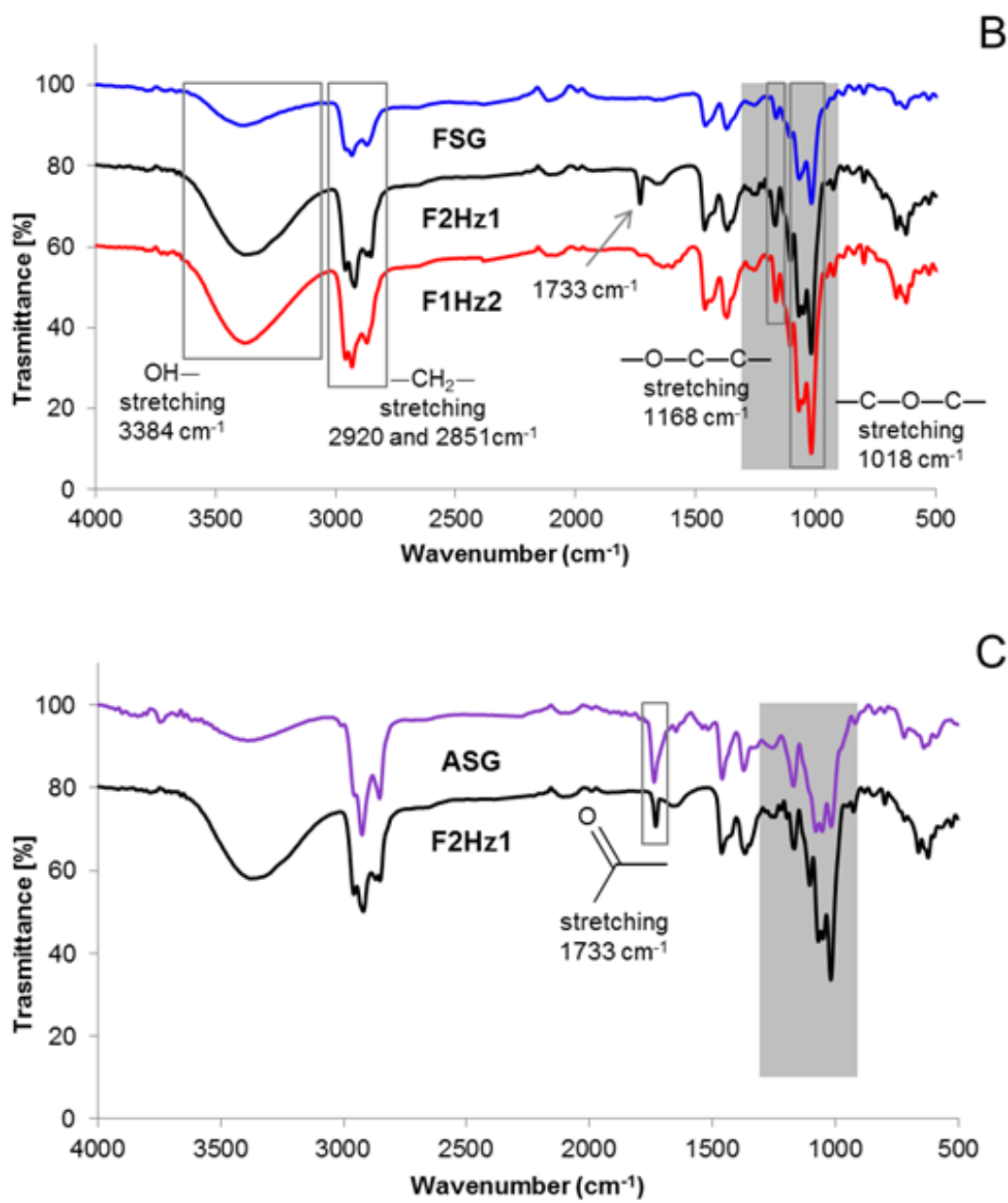


Figure 4. (Continuation)



When ethyl acetate/methanol (10/1 v/v) was used as eluent (Fig. 3B), F1Hz1 and the monopalmitin standard marked a clear and distinct spot at a retention factor of 0.92. In addition, F1Hz2, F2Hz1, and the FSG standard marked a clear and distinct spot at a retention factor of 0.67. This suggested that F1Hz2 and F2Hz1 were

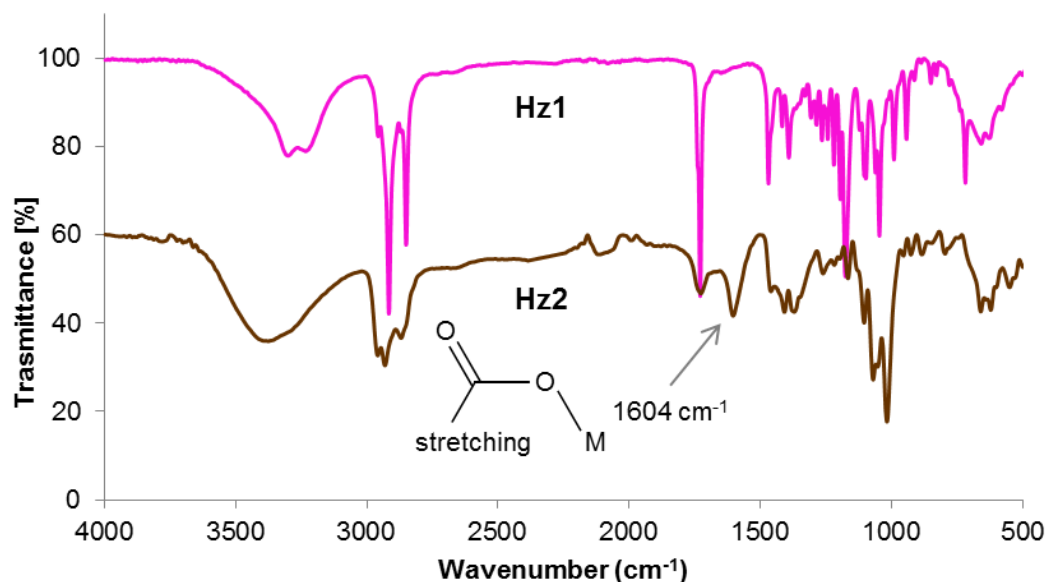
composed of FSG. This finding was consistent with FTIR analysis, where a broad band instead of a doublet of -OH stretching peak (3384 cm^{-1}), less sharp -CH_2 asymmetric and symmetric stretching peaks (2920 and 2851 cm^{-1}), and peaks attributable to asymmetric and symmetric stretching of -C-O-C- (1262 and 1018 cm^{-1}) and asymmetric stretching of -O-C-C- in the glucoside moiety (1168 cm^{-1}) were observed in the spectra of F1Hz2, F2Hz1, and the FSG standard (Fig. 4B). All these signals are characteristic of FSG (Bondioli *et al.*, 2088; Tang *et al.*, 2008b).

An additional peak was observed at 1733 cm^{-1} in the F2Hz1 spectrum. This peak matched the strong peak observed at 1738 cm^{-1} in the ASG standard spectrum (Fig. 4C), and was attributed to stretching of -C=O belonging to the fatty acid chain esterified with the glucoside moiety of ASG (Van Hoed *et al.*, 2008). Since ASG have been demonstrated to coelute with FSG when biodiesel is purified by column chromatography (Lacoste *et al.*, 2009), this finding suggested the presence of ASG in F2Hz1.

Hz1 and Hz2 spectra were virtually the same as F1Hz1 and F1Hz2 spectra, respectively. However, an additional peak was observed at 1604 cm^{-1} in the Hz2 spectrum (Fig. 5). This peak suggested the presence of fatty acid soaps in Hz2. Fatty acid soaps have a peculiar FTIR spectrum, characterized by a strong asymmetrical stretching peak between 1650 and 1550 cm^{-1} (Mirghani *et al.*, 2002). This peak is proper to the two strongly coupled $\text{C}\equiv\text{O}$ bonds forming the carboxylate ion in fatty acid metal salts (Silverstein *et al.*, 2005). Therefore, an additional analysis based on the methylene blue active substances (MBAS) assay was done. MBAS are anionic surfactants capable of forming a 1:1 hydrophobic ion pair with the cationic dye methylene blue. The ion pair is extractable from an acidified aqueous solution into an immiscible organic solvent. MBAS assay comprises successive extractions from acidified aqueous solution containing excess methylene blue into chloroform, followed by colorimetric measurement of the ion

pair in the organic phase by spectrophotometry (Rodier *et al.*, 1998). In accordance with this, 100 mL of deionized water was mixed with 3 g of Hz2 at 20°C for 24 h, then separated from the mixture, and then mixed with 5 mL of acidified aqueous solution of methylene blue. Three successive extractions into chloroform were done, and the absorbance of the chloroform extract was measured using a UV-VIS spectrometer at 650 nm. Thus, the extract tested positive for MBAS, indicating the presence of fatty acid soaps in Hz2.

Figure 5. FTIR spectra of Hz1 and Hz2 in the wavenumber range of 4000-400 cm^{-1} .



2.3.5.2. GC-FID

While FSG were not detected, trace levels of monoglycerides were quantified in the as-received DOPB (Table 8). FSG were also not detected in DPOB spiked with F1Hz1 (Fig. 6A), but monoglycerides content was over six-fold higher than that of DPOB. Monoglycerides content of DPOB spiked with F2Hz1 and F1Hz2 did not change in comparison with DPOB, but FSG content increased, becoming detectable (Fig. 6B and C). Thus, F1Hz1 was confirmed to be composed of

monoglycerides, and F1Hz2 and F2Hz1 were confirmed to be composed of FSG. In addition, one of the main saturated monoglycerides peaks in the GC-FID chromatogram of DPOB spiked with F1Hz1 was identified as monopalmitin (Fig. 7). Thus, F1Hz1 was demonstrated to be mostly composed of monopalmitin, in accordance with the TLC results.

Table 8. Selected properties for DPOB, as received and spiked with F1Hz1, F2Hz1, and F1Hz2.

Property	Unit	DPOB	DPOB-F1Hz1 ^a	DPOB-F2Hz1	DPOB-F1Hz2
FSG content	mg L ⁻¹	N.D. ^b	N.D.	37.6	47.3
MG content	mass%	0.0024	0.0166	0.0022	0.0029
DG content	mass%	N.D.	N.D.	N.D.	N.D.
TG content	mass%	N.D.	N.D.	N.D.	N.D.
Free glycerin content	mass%	0.0084	0.0035	0.0009	0.0032
Total glycerin content	mass%	0.0090	0.0078	0.0015	0.0040

^aDPOB spiked with F1Hz1

^bNot detected

Figure 6. Representative GC-FID chromatograms of DPOB spiked with F1Hz1 (A), F2Hz1 (B), and F1Hz2 (C). Peaks detected in the range of 17.5-18.5 min corresponded to FSG. Limit of detection: 1.9 mg L⁻¹.

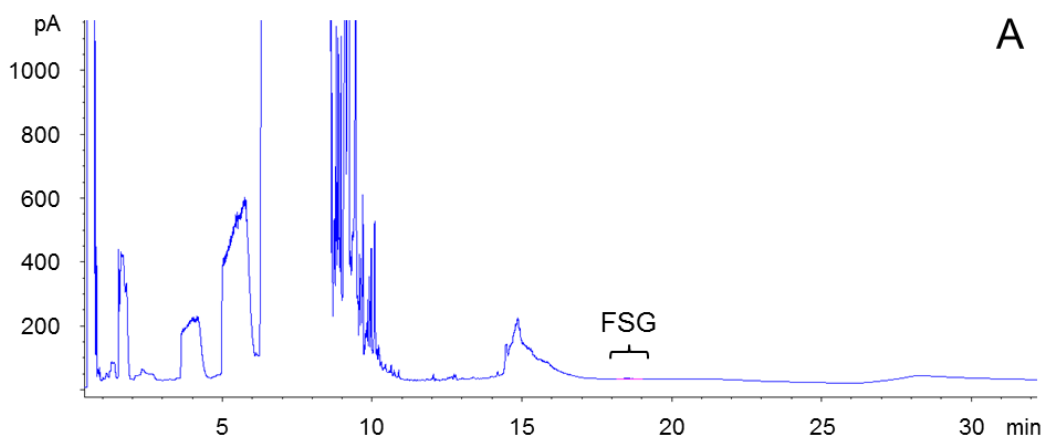
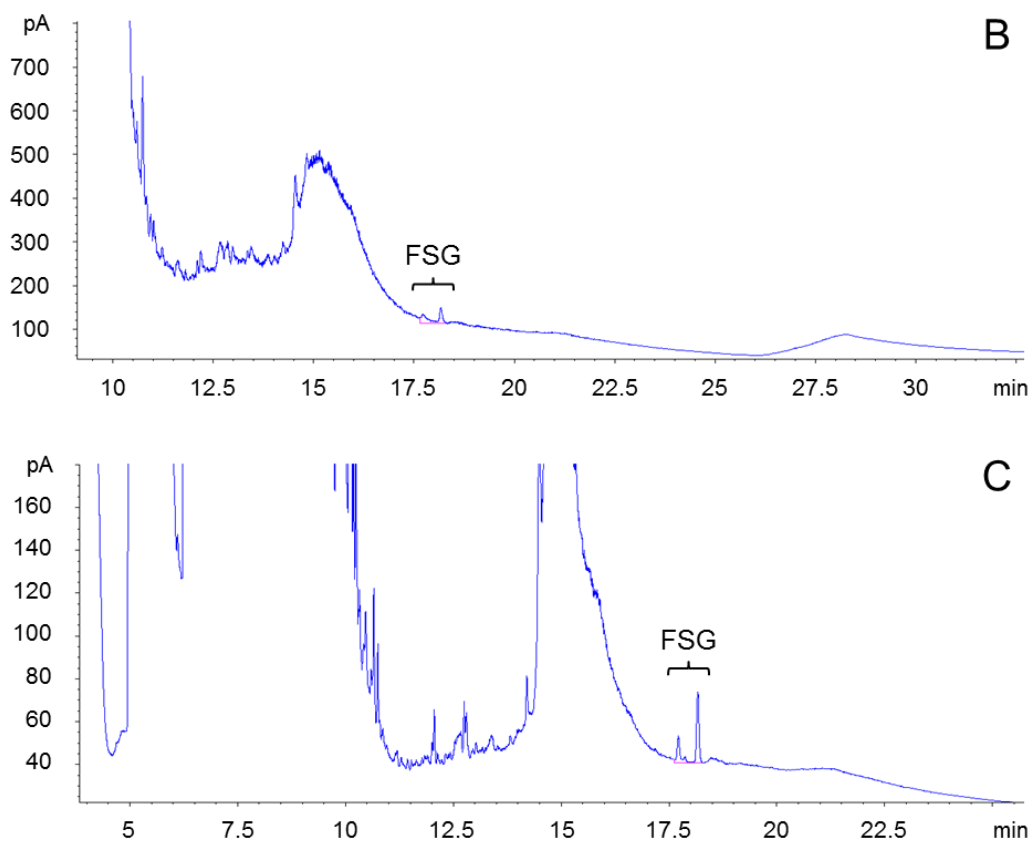


Figure 6. (Continuation)



2.3.5.3. DSC and TGA

A strong endothermic peak was observed in the DSC curve of F1Hz1 and the monopalmitin standard during the heating step (73.81 and 78.60 °C, respectively) (Fig. 8). This peak corresponds to melting of the β form of monopalmitin (Vereecken *et al.*, 2009), indicating that the polymorph in which F1Hz1 precipitated was the β form. Saturated monoglycerides may exist in several polymorphs, namely sub- α , α , and β forms, which have different physical properties; of them, the β form has the highest melting point and is the most stable polymorph (Vereecken *et al.*, 2009). In biodiesel, monopalmitin initially precipitates in one of the low melting polymorphs and transforms into the β form over time during storage (Chupka *et al.*, 2011).

Figure 7. Representative GC-FID chromatogram of DPOB spiked with F1Hz1. Peaks detected at 5.5 and 19.2 min corresponded to the internal standards, namely butanetriol and tricaprin, respectively, while in the range of 9-11 min corresponded to fatty acid esters of the POB and in the range of 14.5-16.8 corresponded to monoglycerides. Peaks represented in red corresponded to a standard mixture of monoglycerides.

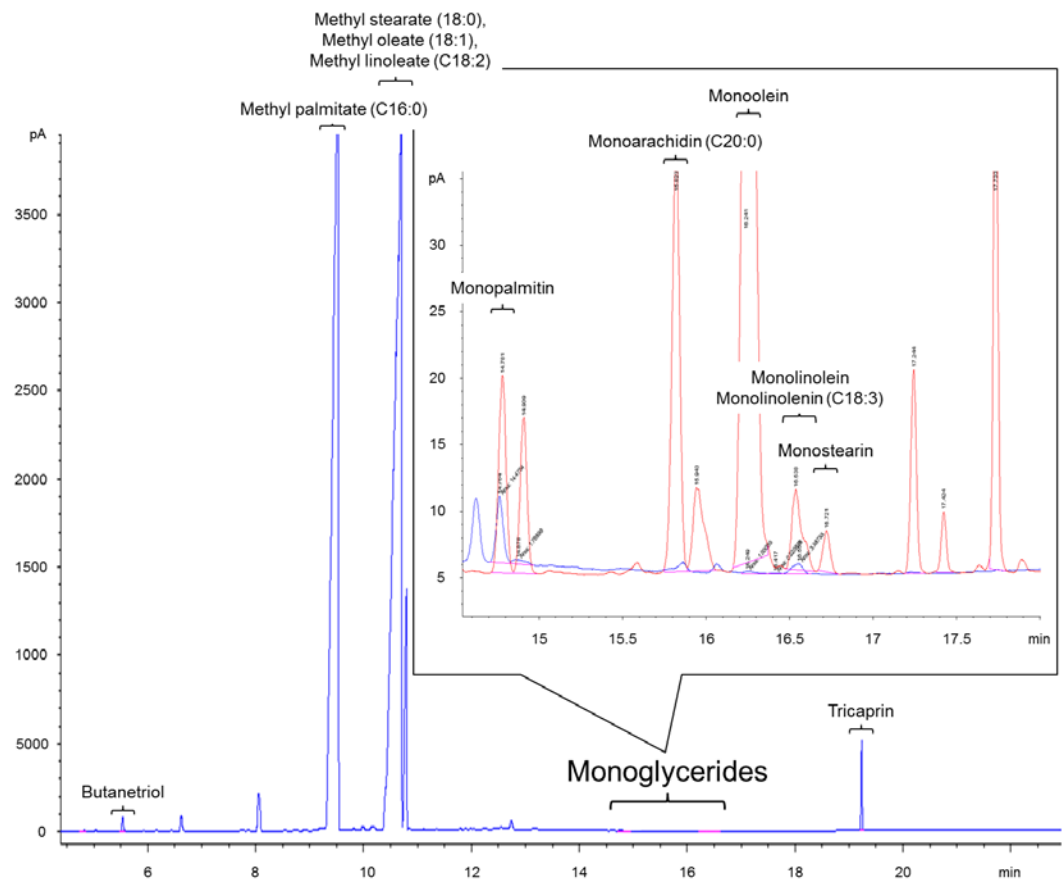
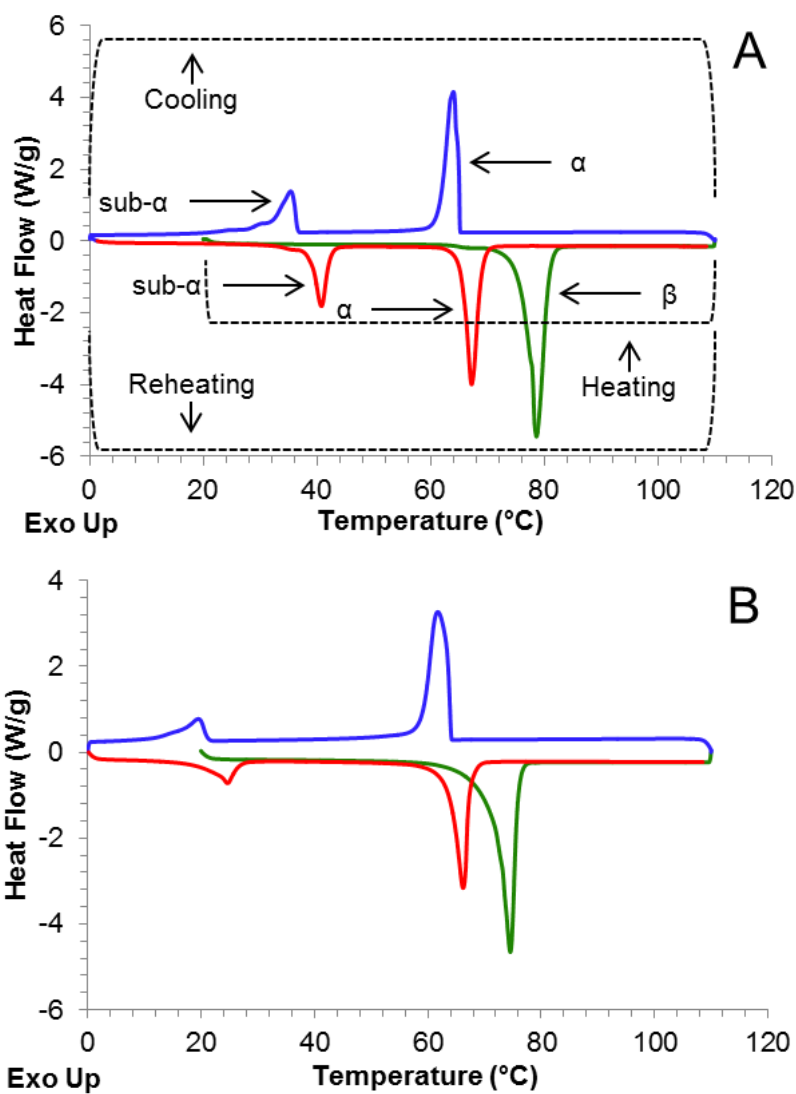


Figure 8. DSC curves of the monopalmitin standard (A) and F1Hz1 (B).



When melted, the β form is not formed again upon cooling; instead, the α form is formed. When sufficiently cooled, the α form undergoes a polymorphic transition to the sub- α form (Vereecken *et al.*, 2009). This is consistent with the exothermic peaks observed for F1Hz1 (62.20 and 19.64 °C) and the monopalmitin standard (63.98 and 35.38 °C) during the cooling step. The pattern observed during the reheating step was completely the same as that observed during the cooling step,

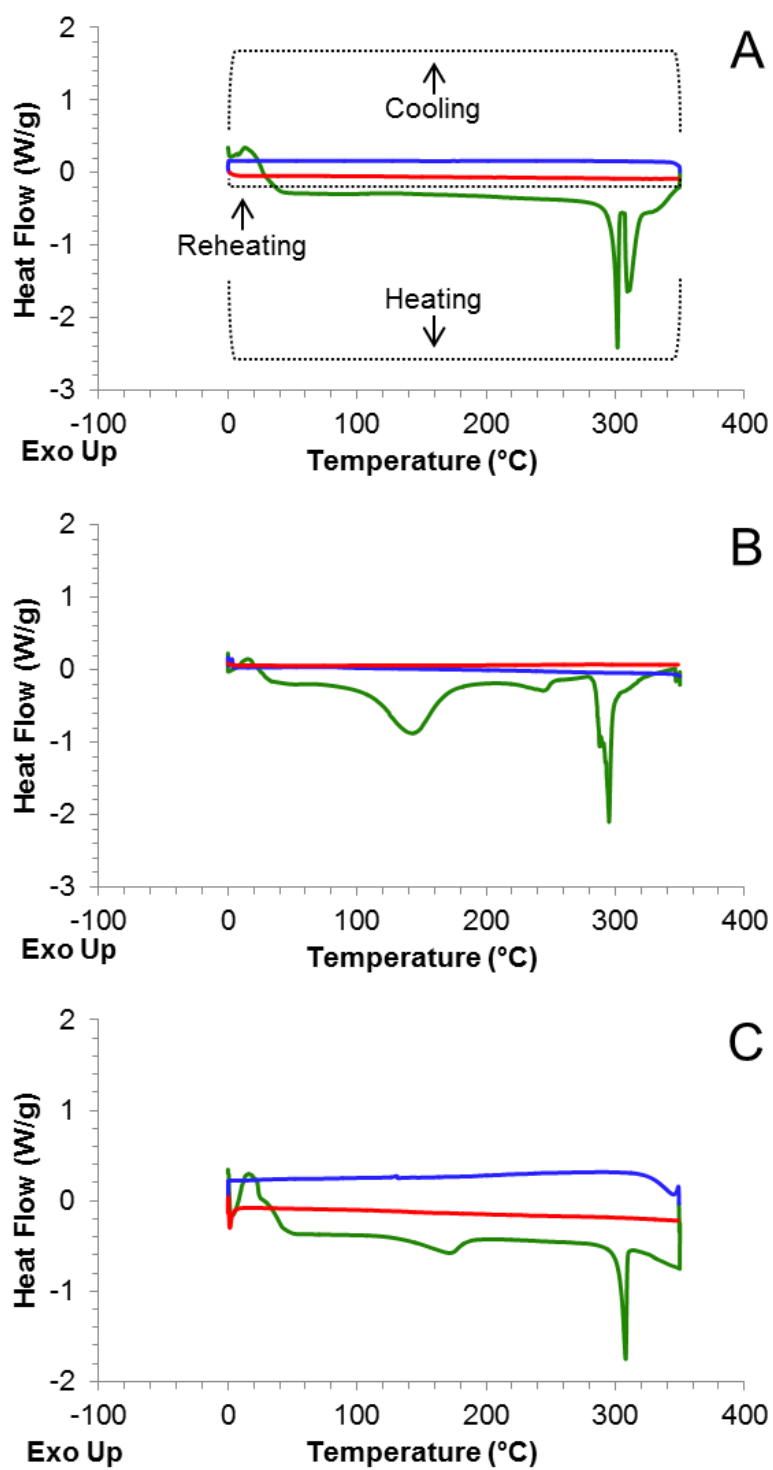
i.e. endothermic peaks for F1Hz1 (24.55 and 65.94 °C) and the monopalmitin standard (40.78 and 67.20 °C), indicating that the polymorphic behavior during the reheating step was completely the same as that during the reheating step. This was in agreement with Vereecken *et al.* (2009).

Peak temperatures were depressed, and peaks were slightly broader. This may have been due to unknown components that may have eluted with the monopalmitin during fractionation by column chromatography and have similar polarity and thermal behavior to the monopalmitin. When present, even at trace levels, impurities displace DSC peak temperatures and impart complex features to melting and crystallization profiles that may not be easy to interpret, such as broad peaks and shoulders not separable from peaks (Romain *et al.*, 2013).

A series of strong endothermic peaks was observed at high temperatures (300-310 °C) in the DSC curve of the FSG standard during the heating step (Fig. 9A). This was followed by the lack of exothermic and endothermic peaks during the cooling and reheating steps, respectively, evidencing that the FSG standard did not undergo a reversible, simple solid to liquid transition, but a decomposition reaction. This was in agreement with Van Gerpen *et al.* (2011).

DSC curves of F2Hz1 and F1Hz2 were virtually the same as that of the FSG standard (Fig. 9B and C), except for a broad endothermic peak observed at lower temperatures (146.55 and 170.09 °C, respectively) during the heating step. This may have been due to unknown components that may have eluted with the FSG during fractionation by column chromatography, have similar polarity to FSG, and underwent thermal decomposition when subjected to temperatures above 300 °C.

Figure 9. DSC curves of the FSG standard (A), F2Hz1 (B), and F1Hz2 (C).



Two consecutive mass losses were observed during TGA of the monopalmitin standard (242.24 and 327.70 °C, Table 9). These mass losses correspond to volatilization that monoglycerides undergo when subjected to temperatures above 150 °C and decomposition that monoglycerides undergo when subjected to temperatures above 300 °C (Fernandes Junior *et al.*, 2012). Similar mass losses were observed during TGA of F1Hz1 (230.82 and 366.89 °C, Table 9), confirming the presence in this fraction of unknown components that may have eluted with the monopalmitin during fractionation by column chromatography, as discussed above, and undergo volatilization and decomposition when subjected to temperatures above 150 °C, such as monomyristin (C14:0) and monostearin (C18:0) (Table 5). Analogous results were reported by Fernandes Junior *et al.* (2012), who characterized precipitates isolated from beef tallow biodiesel using TGA. After checking that the precipitates were composed of monopalmitin and monostearin, the authors observed two mass losses during TGA of all samples (the former above 150 °C and the latter above 300 °C).

Table 9. Representative TGA data of F1Hz1 and the monopalmitin (MP) standard.

Sample	Step	Peak temperature (°C)	Mass loss (%)	Residual mass (%)
MP	1	242.24	89.65	0.49
	2	327.70	9.86	
F1Hz1	1	230.82	59.92	1.38
	2	366.89	38.70	

One mass loss was observed during TGA of the FSG standard (360.68 °C, Table 10). This mass loss correspond to thermal decomposition that FSG undergo when subjected to temperatures above 290 °C, as discussed above. F2Hz1 and F1Hz2 underwent a similar mass loss at 328.75 and 342.01 °C, respectively. Depression of peak temperatures may have been due to the unknown components that may have been eluted with the FSG during fractionation by column chromatography, as discussed above. The unknown components may also have been the cause of the additional mass losses observed during TGA of F2Hz1 and F1Hz2 (148.69 and

131.40 °C, respectively, Table 10), which matched the additional endothermic peaks observed in the DSC curve of these fractions during the heating step. Those components, however, appeared to have undergone some reaction during POB storage, as indicated by the significant reduction in the first mass loss for F1Hz2 (83.12%)

Table 10. Representative TGA data of F2Hz1, F1Hz2, and the FSG standard.

Sample	Step	Peak temperature (°C)	Mass loss (%)	Residual mass (%)
FSG	1	360.68	97.79	2.21
F2Hz1	1	148.69	32.46	
	2	328.75	64.52	3.02
F1Hz2	1	131.40	5.48	
	2	342.01	91.29	3.23

2.4. CONCLUSIONS

Chloroform/methanol (85/15 v/v) was found to be capable of dissolving precipitates isolated from POB for fractionation by column chromatography. Two primary fractions, namely F1Hz1 and F2Hz2, were extracted from the precipitates. The differences in appearance and consistency between the precipitates were mainly attributed to those primary fractions.

Characterization revealed the predominant presence of monopalmitin and FSG in the precipitates. Absorption peaks characteristic of monoglycerides and FSG were observed in the FTIR spectra of F1Hz1 and F1Hz2, respectively, which was consistent with the increase in monoglycerides content of DPOB spiked with F1Hz1 and in FSG content of DPOB spiked with F1Hz2. DSC melting and crystallization profile of F1Hz1 revealed that the monopalmitin precipitated in the β form. FTIR suggested the presence of ASG in F2Hz1 and of fatty acid soaps in Hz2, and thermal analysis revealed the presence of unknown components that may have eluted with the monopalmitin and FSG during fractionation by column

chromatography. All these findings should result in the development of techniques to improve POB filterability not only focused on the removal of FSG from POB.

Depending on the conditions at which the POB was stored, the precipitates consisted mostly of monopalmitin or FSG, confirming that storage conditions significantly impact the constitution of biodiesel precipitate. However, since POB exhibits high oxidative stability (Liang *et al.*, 2006), even under long storage times (Moser, 2011), the precipitates were not expected to contain oxidation byproducts in significant amounts.

3. INFLUENCE OF MINOR COMPONENTS ON PRECIPITATE FORMATION AND FILTERABILITY OF PALM OIL BIODIESEL ⁴

3.1. INTRODUCTION

In last chapter, precipitates isolated from POB were demonstrated to be mostly composed of FSG and monoglycerides, especially monopalmitin (Plata *et al.*, 2015). Because of their limited solubility in biodiesel, researchers have reported that FSG are the main cause of biodiesel precipitate formation (Van Hoed *et al.*, 2008; Lacoste *et al.*, 2009; Bondioli *et al.*, 2008). Monoglycerides result from incomplete conversion of the oils or fats during transesterification and remain in the final biodiesel (Dunn, 2009). Residual monoglycerides may form complexes with FSG, and complexes may interact with moisture, exacerbating precipitate formation (Dunn, 2009).

Only three papers regarding the effect of minor components on biodiesel precipitate formation have been published so far, to the best of our knowledge. Lin *et al.* (2011) examined the effect of saturated monoglycerides, glycerin, and fatty acid soaps on CSFT of canola oil biodiesel and found that none of these minor components at concentrations resembling those that might be encountered in commercial biodiesel caused CSFT to be higher than 360 s. Pfalzgraf *et al.* (2007) and Chupka *et al.* (2012) examined the effect of FSG, monoglycerides, and moisture on CSFT of soybean oil biodiesel, but their results were contradictory. Pfalzgraf *et al.* (2007) found that monoglycerides markedly affected CSFT, but their effect was not comparable to that of FSG. In contrast, Chupka *et al.* (2012) found that FSG did not markedly affect CSFT. Therefore, the primary objective of this chapter was to investigate the effect of FSG, monoglycerides, and moisture

⁴ This chapter is based on the paper "*Influence of minor components on precipitate formation and filterability of palm oil biodiesel*" by Vladimir Plata, Paola Gauthier-Maradei, and Viatcheslav Kafarov, published in Fuel (2015) 144:130-136
<http://dx.doi.org/10.1016/j.fuel.2014.12.043>

content on precipitate formation and filterability of POB. A related objective was to provide statistically significant models to predict CSFT and the precipitate content of POB.

3.2. MATERIALS AND METHODS

3.2.1. Materials

DPOB was supplied by ICP-Ecopetrol. The DPOB was produced in accordance with the ASTM D5236 Standard Test Method. Monopalmitin and monoolein standards were obtained from Nu-Chek Prep, Inc. (Elysian, MN) and were reported to be >99% pure. A FSG standard mixture was obtained from Matreya, Inc. (Pleasant Gap, PA) and was reported to be >98% pure. The composition of the standard mixtures was 56, 25, and 18%, β sitosteryl, campesteryl, and stigmasteryl glucoside, respectively. All solvents were Carlo Erba Reagents (Milan, Italy) ACS reagent grade.

3.2.2. Biodiesel analysis

Fatty acid composition of the as-received DPOB was determined by CROM-MASS at the Industrial University of Santander in accordance with the ISO 5508:1990 and 5509:2000 Standards. Free and total glycerin content (mass fraction) of the DPOB was determined in accordance with the ASTM D6584 Standard Test Method. FSG content was determined using the ICP CLR-CRO-I-091 procedure. These analyses were done by the Chromatography Laboratory at ICP-Ecopetrol.

3.2.3. Preparation of biodiesel samples

Before adding the minor components, the DPOB was dried using sodium sulfate, and then filtered. One portion of the dried biodiesel was humidified by coming into contact with deionized water for 48 h, and the other portion was stored under an inert atmosphere. Moisture content of the dried and humidified biodiesel was measured following the ASTM E203 Standard Test Method. A 1500 mg L⁻¹ FSG

stock solution was prepared in chloroform/methanol (85/15, v/v). A calculated volume of this solution was added to an adequate volume of dried biodiesel via pipette, and the resulting mixture was heated at 65 °C and 7 kPa for 2 h to evaporate the chloroform/methanol introduced by the stock solution. A calculated mass of monopalmitin and monoolein standards was weighed using a Precisa XB 220A analytical balance, and then quantitatively transferred to a 500 mL bottle where an adequate volume of humidified biodiesel was added. The standards were mixed to the proportions of saturates and unsaturates of typical POB fatty acid composition (50.8 and 49.7 mass%, respectively, Prada *et al*, 2011). Dissolution of the standards into the humidified biodiesel was aided by heating at 65 °C for 1 h. Once evaporation and dissolution finished, dried and humidified DPOB containing the minor components were blended with each other to get a 300 mL sample. The resulting sample was immediately held at 40 °C for 3 h under an inert atmosphere, and then at 25 °C for 24 h, before the cold soak filtration test. Detailed amounts of FSG stock solution, monopalmitin and monoolein standards, and dried and humidified biodiesel blended to prepare the 300 mL spiked samples are provided in Table 11.

3.2.4. Cold soak filtration test

The cold soak filtration test was performed in accordance with the ASTM D7501 Standard Test Method. After soaking at 4 °C for 16 h, the 300 mL samples were allowed to warm to 25 °C in a water bath and held at this temperature for 4 h. The samples were then filtered through a 0.7 µm glass microfiber filter (Whatman GF/F, 47 mm diameter, Piscataway, NJ) under 70 to 80 kPa of vacuum. ASTM D7501 filtration apparatus comprises a funnel, a funnel base with a filter support, the glass microfiber filter, and a receiving flask assembled as a unit by a clamp. The time required for the biodiesel to pass through the glass microfiber filter was recorded as CSFT. The amount of precipitate retained on the glass microfiber filter was determined in accordance with the ASTM D7321 Standard Test Method with minor modifications. After filtration, the sample container was rinsed with *n*-heptane

previously filtered through a 0.45 μm glass microfiber filter (Millipore AP40, 47 mm diameter, Billerica, MA), and the rinses were poured into the funnel and filtered through the glass microfiber filter. Similarly, the funnel was rinsed, and the rinses were filtered. With the vacuum applied, the funnel was carefully separated from the funnel base, and the periphery of the glass microfiber filter was washed with *n*-heptane by directing a gentle stream from the edge to the center. The vacuum was maintained for 10 to 15 s after washing to remove excess *n*-heptane from the glass microfiber filter. Using clean forceps, the glass microfiber filter was carefully removed from the filter support, and then dried in an oven at 110 °C for 30 min, in contrast to the ASTM D7321 Standard Test Method where the drying temperature is 90 °C. When cooled, the glass microfiber filter was weighed, and the mass was recorded to the nearest 0.1 mg. The precipitate content was calculated from the increase in the mass of the glass microfiber filter and was reported in mg L^{-1} .

Table 11. Amounts of FSG stock solution, monopalmitin and monoolein standards, humidified and dried biodiesel blended to prepare the 300 mL spiked DPOB samples.

Treatment	Monopalmitin (g)	Monoolein (g)	FSG stock (μL)	DPOB ^a (g)	DPOB ^b (g)
1	0.1578	0.1422	2927	52.78	211.30
2	0.1578	0.1422	8780	52.78	211.30
3	0.4732	0.4268	2927	52.78	211.30
4	0.4732	0.4268	8780	52.78	211.30
5	0.1578	0.1422	2927	193.53	70.55
6	0.1578	0.1422	8780	193.53	70.55
7	0.4732	0.4268	2927	193.53	70.55
8	0.4732	0.4268	8780	193.53	70.55
9	0.3155	0.2845	931	123.16	140.92
10	0.3155	0.2845	10776	123.16	140.92
11	0.0502	0.0453	5854	123.16	140.92
12	0.5808	0.5237	5854	123.16	140.92
13	0.3155	0.2845	5854	4.80	259.28
14	0.3155	0.2845	5854	241.42	22.66
15, 16, 17	0.3155	0.2845	5854	123.16	140.92

^aHumidified DPOB, moisture content = 1328 mg L^{-1}

^bDried DPOB, moisture content = 183 mg L^{-1}

3.2.5. Experimental design

A three-factor, five level central composite design (CCD) was conducted to examine the combined effect of FSG, monoglycerides, and moisture content on CSFT and the precipitate content. CCD has the advantage of predicting a response based on a few sets of experimental data, in which independent factors vary within a fixed range (Gutiérrez Pulido and De la Vara Salazar, 2008). CCD consists of the standard 2^k factorial points, a replicated center point, and $2k$ points fixed axially at a distance from the center given by the general formula $\alpha = 2^{k/4}$, where k is the number of factors. For three factors, α is equal to 1.682, which makes the design rotatable. Three replicates of the center point were used to determine the experimental error and the reproducibility of the data. Thus, a set of 17 treatments including 8 factorial points, 6 axial points, and 1 center point replicated three times was carried out in randomized order to minimize the effects of uncontrolled factors.

The actual levels of the axial points were calculated using Eq. (1):

$$\alpha_i = \frac{x_i - x_0}{x} \quad (1)$$

where α_i represents the coded value, x_i represents the actual value, x_0 represents the average value of the factor in low (-1) and high (+1) levels and x may be calculated as follows:

$$x = \frac{\text{Factor in high level} - \text{Factor in low level}}{2} \quad (2)$$

The high (+1) level of FSG was fixed at 30 mg L⁻¹ because biodiesel filterability may be affected even when FSG content is as low as 20 mg L⁻¹ (Lacoste *et al.*, 2009). The high (+1) level of monoglycerides was fixed at 0.3 mass% because this is the usual level of monoglycerides in Colombian commercial POB, according to

historical records from Ecodiesel Colombia S.A. The high (+1) level of moisture were fixed well above the 500 mg L⁻¹ limit specified in the European Standard EN 14214 to consider that biodiesel may absorb moisture during storage and transit.

Multiple regression analysis was used to fit the response values by the second-order polynomial model:

$$y = \beta_o + \sum_{i=1}^n \beta_i x_i + \sum_{i=1}^{n-1} \sum_{j=i+1}^n \beta_{ij} x_i x_j + \sum_{i=1}^n \beta_{ii} x_i^2 \quad (3)$$

where Y represents the predicted response, β_o represents the constant coefficient, β_i represents the linear effect, β_{ij} represents the interaction effect, β_{ii} represents the squared effect, and x_i and x_j represent the independent factors. The model was satisfactory when ANOVA showed a high statistical significance (p -value <0.05). Regression coefficients were also tested for statistical significance. Statgraphics Centurion software (free trial version, StatPoint Technologies, Inc., Warrenton, VA) was employed to determine the regression coefficients and perform the ANOVA. Response surfaces were generated using the fitted second-order polynomial model, holding one of the factors at a constant level corresponding to the middle level and changing the other two factors. Confirmatory experiments were carried out using 3 combinations of factors that were not part of the original CCD treatments, but within the design space. The confirmatory experiments involved preparation of spiked biodiesel followed by cold soak filtration test of the resulting samples as described above.

3.3. RESULTS AND DISCUSSION

3.3.1. Biodiesel analysis

Methyl palmitate (C16:0) and methyl oleate (C18:1) were the primary fatty acid esters of the as-received DPOB (Table 12) along with methyl linoleate (C18:2) and methyl stearate (C18:0). This, along with the proportions of saturates (49.5

mass%) and unsaturates (50.3 mass%), was consistent with the fatty acid composition typical for POB (Prada *et al.*, 2011), indicating that the main composition of the DPOB was similar to that of POB.

While diglycerides and triglycerides were not detected, trace levels of monoglycerides and glycerin were quantified in the DPOB (Table 13); however, the levels were below the limit above which these minor components may have a significant effect on precipitate formation (Lin *et al.*, 2011). FSG were also not detected in the DPOB (Fig. 10A), but spiking with the FSG stock solution made the FSG detectable (Fig. 10B). Moisture content of the humidified DPOB was well above the EN 14214 limit, consistent with the fact that biodiesel is highly hygroscopic (Alleman and McCormick, 2008).

Table 12 Fatty acid composition of as-received DPOB in comparison with that of typical POB (Prada *et al.*, 2011).

Fatty acid	DPOB (mass%)	POB (mass%)
C14:0	1.0	1.1
C16:0	44.0	44.9
C16:1	0.1	1.3
C18:0	3.9	4.8
C18:1	41.2	36.8
C18:2	8.8	11.3
C18:3	0.2	0.3
C20:0	0.4	N.R. ^a
C22:0	0.1	N.R.
C24:0	0.1	N.R.
ΣSFA^b	49.5	50.8
ΣUFA^c	50.3	49.7

^aNot reported

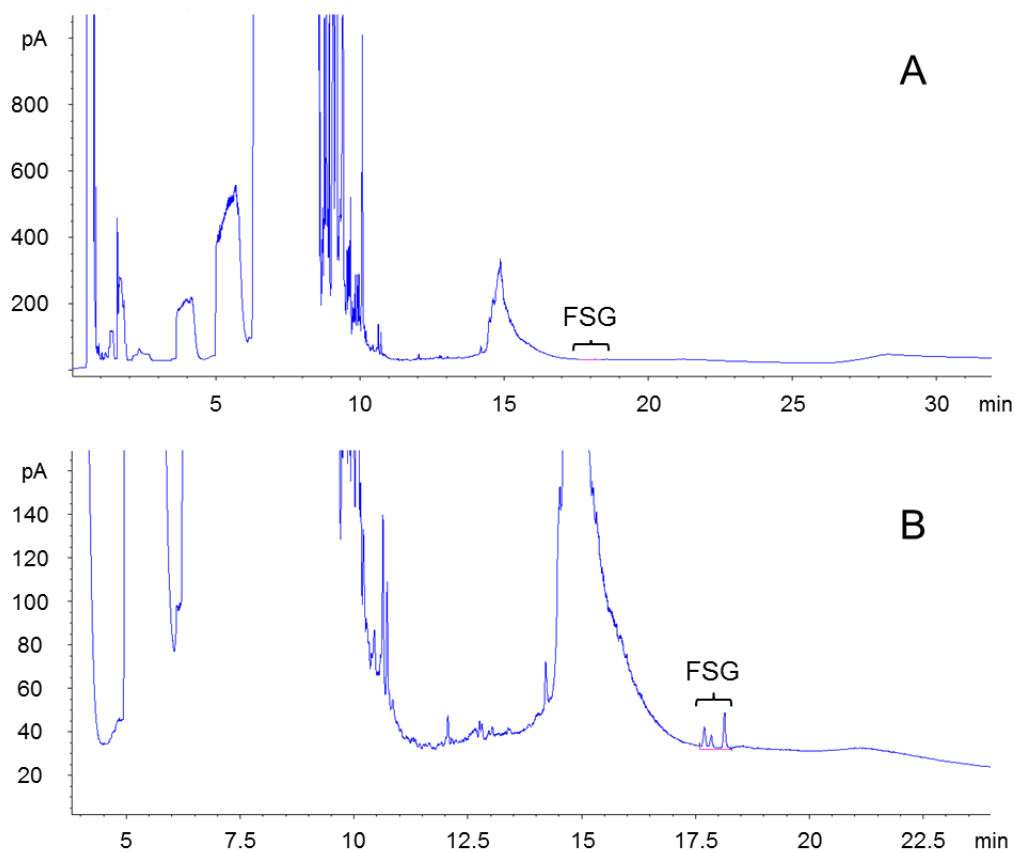
^b $\Sigma SFA = C14:0 + C16:0 + C18:0 + C20:0 + C22:0 + C24:0$

^c $\Sigma UFA = C16:1 + C18:1 + C18:2 + C18:3$

Table 13. Selected properties for as-received and humidified DPOB.

Property	EN limit	Unit	DPOB	DPOBh
MG content	0.80	mass%	0.0024	-
DG content	0.20	mass%	N.D.	-
TG content	0.20	mass%	N.D.	-
Free glycerin content	0.02	mass%	0.0084	-
FSG content	N.S.	mg L ⁻¹	N.D.	-
Moisture content	500	mg L ⁻¹	-	1328

Figure 10. Representative GC-FID chromatograms of non-spiked DPOB (A) and DPOB spiked with FSG (30 mg L⁻¹) (B). Peaks detected in the range of 17.5-18.5 min corresponded to FSG. Limit of detection: 1.9 mg L⁻¹.



3.3.2. Model fitting

The response values from the CCD experiments conducted to examine the combined effect of FSG (x_1), monoglycerides (x_2), and moisture (x_3) on CSFT (Table 14) were fitted to the second-order polynomial model described in Eq. (3) using multiple regression analysis. The resulting model was not statistically significant, according to the ANOVA results (p -value = 0.0650). Only three coefficients were significant, namely x_1 , x_2^2 , and x_3^2 (p -value = 0.0104, 0.0326, and 0.0106, respectively). Therefore, new regression analyses removing the insignificant coefficients one at a time were done to obtain a better model; however, x_3 was kept due to the significance of the squared coefficient x_3^2 . After removing the three most insignificant coefficients, namely x_2 , x_1x_2 , and x_2x_3 (p -value = 0.8736, 0.7324, and 0.4883, respectively), a statistically significant model was obtained (p -value = 0.0058). The model is given in Eq. (4) (in terms of coded values).

The goodness of fit was evidenced by the reasonably high coefficient of determination of the model ($R^2 = 0.7903$), indicating that 80% of the response variability can be explained by the model, and therefore the model can be used for prediction within the design space with reasonable precision (Gutiérrez Pulido and De la Vara Salazar, 2008). Additional regression analyses removing the rest of insignificant coefficients were not successful because the p -value of the resulting models increased (p -value = 0.0063 and 0.0057, respectively) and the coefficient of determination decreased ($R^2 = 0.7332$ and 0.7380, respectively). Thus, the model given in Eq. (4) was found as the best for prediction of CSFT within the design space.

Table 14. Central composite design examining the effect of FSG, monoglycerides (MG), and moisture content on CSFT and the precipitate content of POB.

Treatment	Level of factors, actual (coded)			CSFT (s)	Precipitate content (mg L ⁻¹)
	FSG content, x_1 (mg L ⁻¹)	MG content, x_2 (mass%)	Moisture content, x_3 (mg L ⁻¹)		
1	10 (-1)	0.1 (-1)	265 (-1)	100	75
2	30 (+1)	0.1 (-1)	265 (-1)	230	101
3	10 (-1)	0.3 (+1)	265 (-1)	92	52
4	30 (+1)	0.3 (+1)	265 (-1)	185	64
5	10 (-1)	0.1 (-1)	973 (+1)	117	91
6	30 (+1)	0.1 (-1)	973 (+1)	158	89
7	10 (-1)	0.3 (+1)	973 (+1)	127	68
8	30 (+1)	0.3 (+1)	973 (+1)	169	78
9	3 (- α)	0.2 (0)	619 (0)	77	79
10	37 (+ α)	0.2 (0)	619 (0)	168	100
11	20 (0)	0.03 (- α)	619 (0)	143	83
12	20 (0)	0.37 (+ α)	619 (0)	175	43
13	20 (0)	0.2 (0)	24 (- α)	102	68
14	20 (0)	0.2 (0)	1214 (+ α)	95	82
15	20 (0)	0.2 (0)	619 (0)	214	78
16	20 (0)	0.2 (0)	619 (0)	274	79
17	20 (0)	0.2 (0)	619 (0)	169	73

$$Y = 217.3 + 33.61x_1 - 3.498x_3 - 28.30x_1^2 - 15.40x_2^2 - 36.79x_3^2 - 17.50x_1x_3 \quad (4)$$

The response values from the CCD experiments conducted to examine the combined effect of FSG, monoglycerides, and moisture on the precipitate content (Table 14) were also fitted to the second-order polynomial model described in Eq. (3) using multiple regression analysis. According to the ANOVA results, most coefficients were statistically significant, except for x_1x_2 and x_3^2 (p -value = 0.8652 and 0.8319, respectively). Both of them were removed from the model, and the resulting model is given in Eq. (5) (in terms of coded values).

$$Y = 76.24 + 5.954x_1 - 11.81x_2 + 4.214x_3 + 4.941x_1^2 - 4.428x_2^2 - 3.750x_1x_3 + 3.250x_2x_3 \quad (5)$$

This model was highly statistically significant (p -value <0.0001), and its high coefficient of determination ($R^2 = 0.9687$) indicated that more than 96% of the response variability can be explained by the model, and therefore the model can be used for prediction within the design space with high precision.

Fig. 11 shows the measured versus predicted values for the precipitate content. The predicted values were quite close to the measured values, confirming that the model given in Eq. (5) was successful in capturing the correlation between FSG, monoglycerides, and moisture content and the precipitate content. The predicted values for CSFT, for their part, were slightly scattered around the solid line that indicates perfect correlation with the measured values (Fig. 12). However, this scattering should not be interpreted as a lack of suitability of the model given in Eq. (4) to capture the correlation between FSG, monoglycerides, and moisture content and CSFT, given the reasonably high coefficient of determination reported above ($R^2 = 0.7903$).

3.3.3. Model validation

Good agreement was shown to exist between the predicted CSFT and precipitate content values and the measured values from confirmatory experiments (Table 15). No marked differences were observed, and the average deviations were 11.1 and 3.4%. This validated the models given in Eqs. (4) and (5) within the design space.

Figure 11. Measured precipitate contents versus values predicted by the regression model given in Eq. (5).

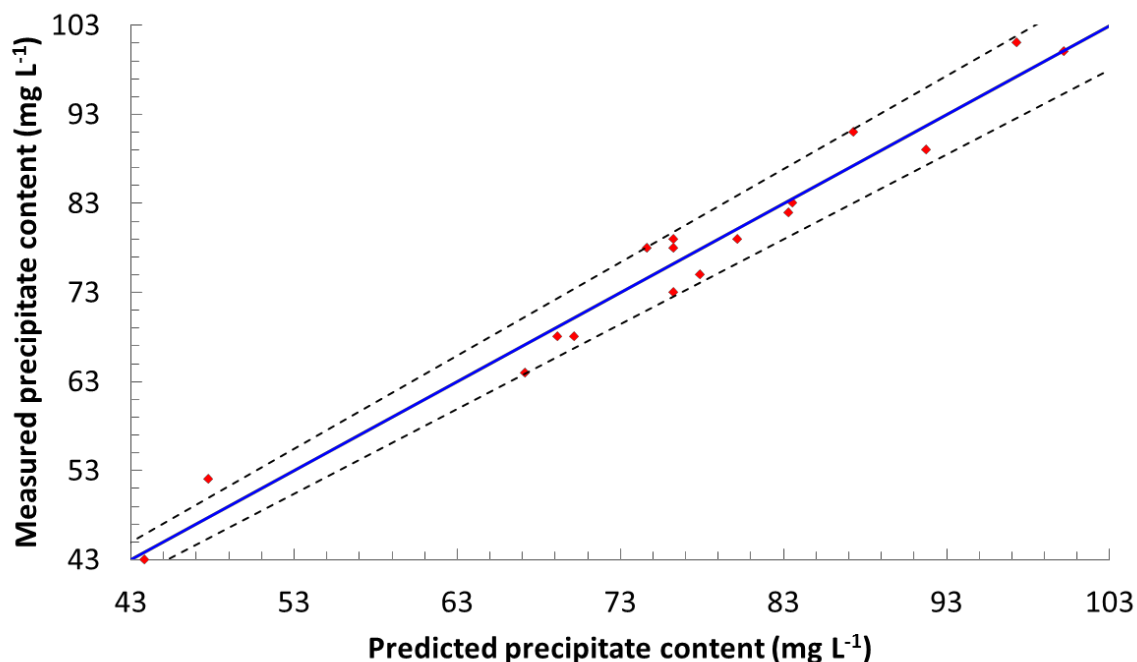
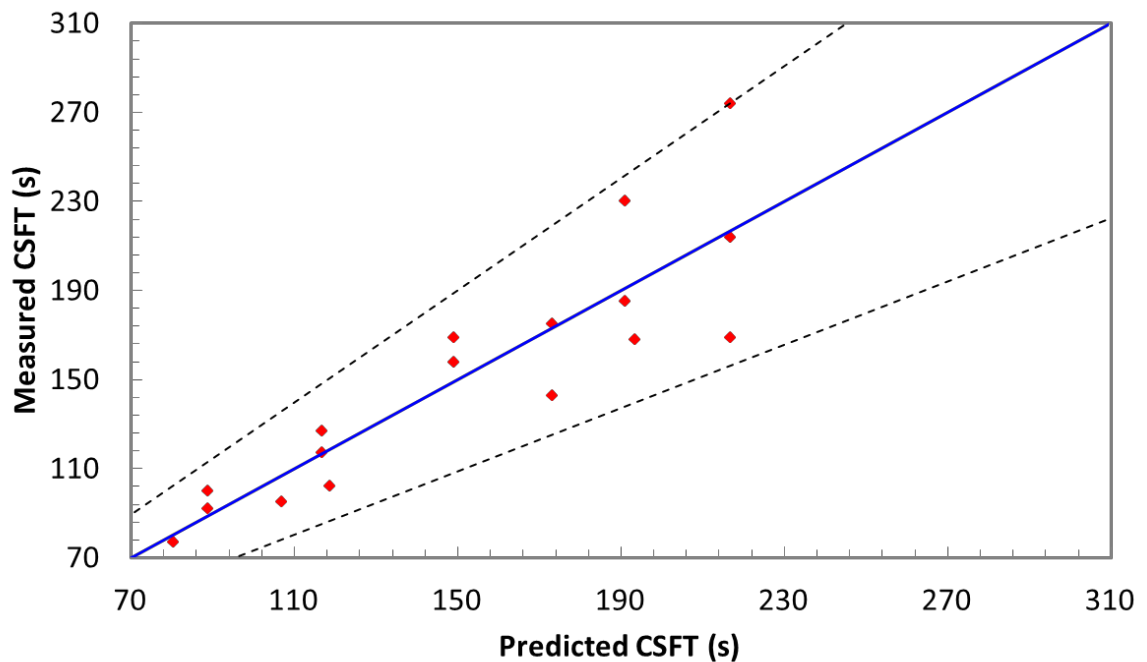


Table 15. Confirmatory experiments to validate the regression model predictions for CSFT and the precipitate content of POB, given FSG, monoglycerides (MG), and moisture content.

FSG content (mg L ⁻¹)	MG content (mass%)	Moisture content (mg L ⁻¹)	CSFT (s)			Precipitate content (mg L ⁻¹)		
			Pred.	Meas.	Dev. (%)	Pred.	Meas.	Dev. (%)
30	0.1	619	207	225	8.6	94	96	1.6
20	0.2	973	177	189	6.8	80	84	4.4
10	0.2	265	105	86	17.8	67	70	4.1

Figure 12. Measured CSFT versus values predicted by the regression model given in Eq. (4).



3.3.4. Effect of FSG, monoglycerides, and moisture

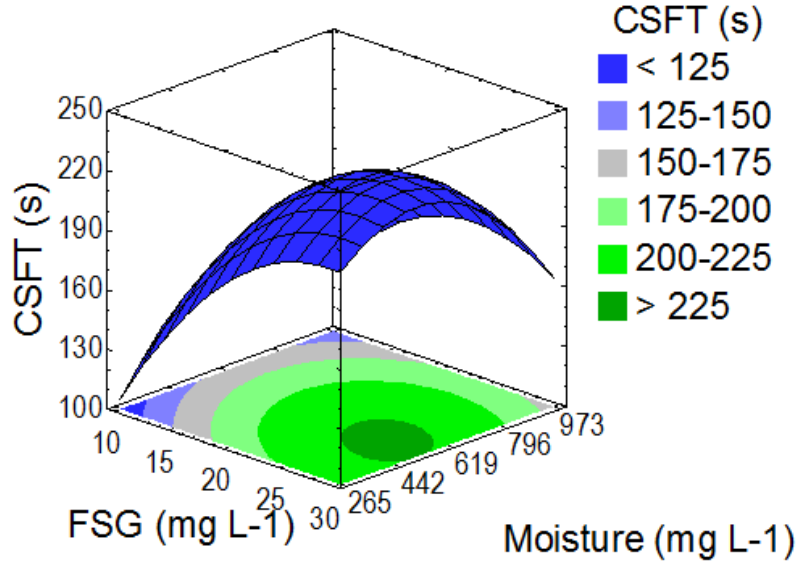
In the CCD experiments conducted to examine the combined effect of FSG, monoglycerides, and moisture on CSFT and the precipitate content (Table 14), all samples met the 360 s limit specified in the ASTM D6751 Standard Specification, indicating that no combination of factors within the design space affected POB filterability even though a large variation in the precipitate content was observed (between 43 and 101 mg L⁻¹, treatments 12 and 2, respectively). As noted above, the high (+1) level of monoglycerides was fixed at 0.3 mass% because this is the usual level of monoglycerides in Colombian commercial POB, and the high (+1) level of moisture was fixed well above the EN 14214 limit to consider that biodiesel may absorb moisture during storage and transit. Therefore, these results suggest that the reduction of FSG content to below 30 mg L⁻¹ may contribute to improve the filterability of commercial POB and that the increase in moisture content that may occur during storage and transit of biodiesel may not represent a risk for

commercial POB filterability, provided that FSG content is lower than 30 mg L⁻¹, monoglycerides content is lower than 0.3 mass%, and the biodiesel does not contain other minor components such as fatty acid soaps in significant amounts.

FSG was the only significant factor affecting CSFT within the design space, according to the ANOVA results (p -value = 0.0023). In contrast, FSG, monoglycerides, and moisture significantly affected the precipitate content (p -value = 0.0002, <0.0001, and 0.0018, respectively). Interaction of FSG and monoglycerides with moisture was also significant on the precipitate content (p -value = 0.0155 and 0.0297, respectively), but interaction between FSG and monoglycerides was not significant, as reported above.

CSFT increased with increasing FSG content and reached a maximum value at certain point, regardless of the moisture content (Fig. 13). Beyond this point, CSFT slightly decreased. The increase in CSFT was probably due to an increase in the precipitate content, in accordance with the modified cake filtration, Eq. (6); this equation has been recognized as a useful tool for understanding the effect of contaminants (minor components) on CSFT (Lin *et al.*, 2011).

Figure 13. Response surface of the combined effect of FSG and moisture on CSFT of POB. The third factor was held at the middle level in generating this plot (monoglycerides, 0.2 mass%).



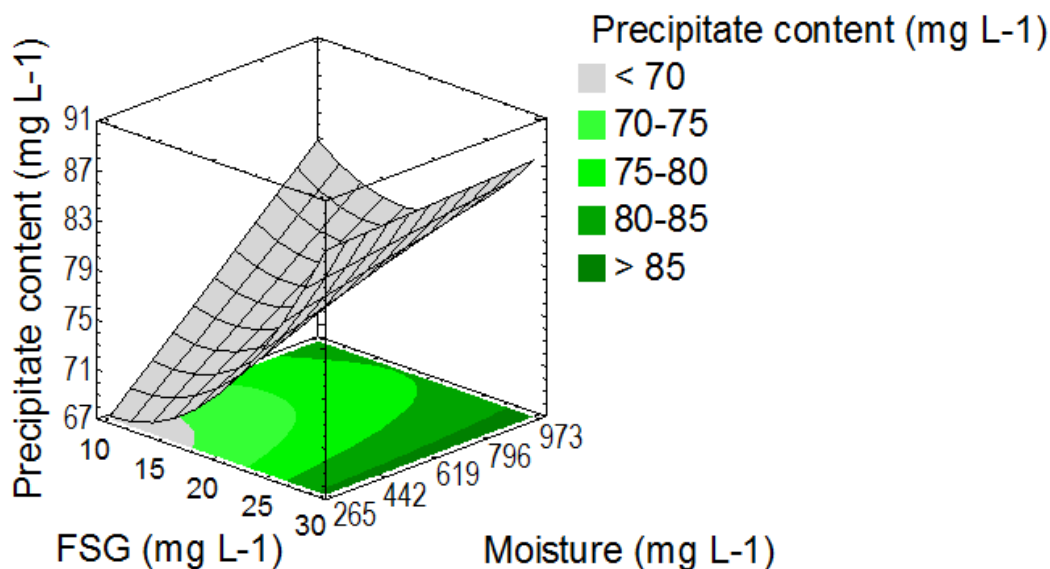
$$CSFT = \frac{\alpha \mu V_b^2}{2 \Delta p A^2} c + \frac{R_f \mu V_b}{\Delta p A} \quad (6)$$

α (m kg^{-1}) represents the specific resistance of the cake; μ (Pa s) represents the dynamic viscosity of the filtrate; c (kg m^{-3}) represents the cake mass per unit volume of filtrate; Δp (Pa) represents the pressure difference across the cake; A (m^2) represents the effective surface area of the glass microfiber filter; V_b (m^3) represents the biodiesel volume; and R_f (m^{-1}) represents the resistance from the glass microfiber filter. All parameters in Eq. (6) are held constant during the cold soak filtration test except α , μ , and c , which may be impacted by the biodiesel minor components; of these three parameters, a change in c is the most expected to cause a marked change in CSFT (Lin *et al.*, 2011).

The precipitate content indeed markedly increased with increasing FSG content at low levels of moisture (Fig. 14), but it slightly decreased and then increased at high

levels of moisture. No reason can be given for this at the moment. Despite this, CSFT still increased (Fig. 13), perhaps because precipitate capable of plugging the glass microfiber filter was formed during cold soak. Depending on the precipitate size and shape, plugging of the glass microfiber filter may occur during the cold soak filtration test even though a small amount of precipitate has been formed during cold soak (Chupka *et al.*, 2012).

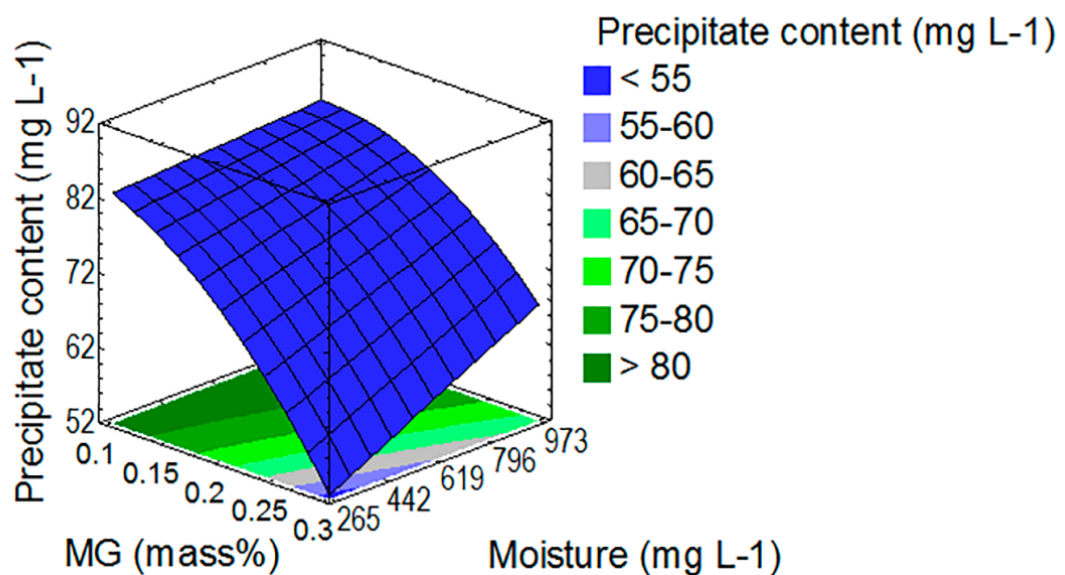
Figure 14. Response surface of the combined effect of FSG and moisture on the precipitate content of POB. The third factor was held at the middle level in generating this plot (monoglycerides, 0.2 mass%).



The precipitate content decreased with increasing monoglycerides content (Fig. 15). Smaller-sized precipitate may have been formed at high levels of monoglycerides, and this precipitate may have been less retained on the glass microfiber filter. This effect, however, was less pronounced at high levels of moisture, confirming that moisture contributes to exacerbate precipitate formation. Monoglycerides are amphiphilic in nature and may interact with moisture to form larger precipitate that may be easier to retain on the glass microfiber filter (Dunn, 2009). This effect was also observed for interaction between FSG and moisture,

i.e. the higher the moisture content, the higher the precipitate content, regardless of the FSG content (Fig. 14). Because of the polarity difference between their hydrophobic sterol and their hydrophilic glucose moieties, FSG also have an amphiphilic structure (Nyström et al., 2012).

Figure 15. Response surface of the combined effect of monoglycerides (MG) and moisture on the precipitate content of POB. The third factor was held at the middle level in generating this plot (FSG, 20 mg L⁻¹).



3.4. CONCLUSIONS

Central composite design and multiple regression analysis were successful in studying the effect of FSG, MG, and moisture content on precipitate formation and filterability of POB. A statistically significant model (p -value = 0.0058) for prediction of CSFT and a highly statistically significant model (p -value < 0.0001) for prediction of the precipitate content, given FSG, monoglycerides, and moisture content, were obtained. FSG was the only significant factor affecting CSFT within the design space whereas FSG, monoglycerides, and moisture significantly affected the precipitate content. Interaction of FSG and monoglycerides with moisture was also

significant on the precipitate content, but interaction between FSG and monoglycerides was not significant.

CSFT increased with increasing FSG content and reached a maximum value at certain point beyond which CSFT slightly decreased. This was probably due to the increase in the precipitate content with increasing FSG content observed at low levels of moisture or the formation of precipitate capable of plugging the glass microfiber filter during the cold soak filtration test. The precipitate content decreased with increasing monoglycerides content. This effect was less pronounced at high moisture contents, confirming that moisture contributes to exacerbate precipitate formation. This effect was also observed for interaction between FSG and moisture.

The reduction of FSG content to below 30 mg L^{-1} may contribute to improve the filterability of commercial POB, and the increase in moisture content that may occur during storage and transit of biodiesel may not represent a risk for commercial POB filterability, provided that FSG content is lower than 30 mg L^{-1} , monoglycerides content is lower than 0.3 mass%, and the biodiesel does not contain other minor components such as fatty acid soaps in significant amounts.

4. IMPROVEMENT OF PALM OIL BIODIESEL FILTERABILITY BY ADSORPTION METHODS⁵

4.1. INTRODUCTION

Although FSG may be significantly removed during refining of vegetable oils (Murui and Siew, 1997), ASG may be converted to FSG during transesterification, resulting in an increased FSG content in biodiesel in comparison with the initial amount in the feedstock oil (Van Hoed *et al.*, 2008). Although monoglycerides content is restricted to trace levels by the ASTM D6751 Standard Specification and European Standard EN 14214, monoglycerides remaining in the final biodiesel may form complexes with FSG, and complexes may interact with moisture, exacerbating precipitate formation (Dunn, 2009). Thus, post-processing techniques for precipitate removal, especially removal of FSG, are needed to improve biodiesel filterability.

Tang *et al.* (2010) examined room temperature and cold soak filtration, treatment with diatomaceous earth, centrifugation, and vacuum distillation, and found that vacuum distillation was the most effective technique to decrease the FSG content in soybean biodiesel. However, drawbacks of vacuum distillation include increased energy consumption, increased capital and operational costs, and reduced yield (Smith, 2012). Several authors claimed the use of adsorbents on biodiesel refining (Lee *et al.*, 2007; Danzer *et al.*, 2011; Na-Ranong *et al.*, 2015); however, little or no characterization of the treated biodiesel was presented. Thus, the primary objective of this chapter was to improve POB filterability through selection of an adsorbent capable of substantially decreasing the precipitate content. Related objectives were to examine the effect of adsorbent treatment on several ASTM D6751

⁵ This chapter is based on the paper "*Improvement of palm oil biodiesel filterability by adsorption methods*" by Vladimir Plata, Darrin Haagenon, Ayhan Dağdelen, Dennis Wiesenborn, and Viatcheslav Kafarov, published in *Journal of the American Oil Chemists' Society* (2015) 92:893-903
<http://dx.doi.org/10.1007/s11746-015-2646-z>

biodiesel properties and to optimize the operational conditions of the adsorbent treatment.

4.2. MATERIALS AND METHODS

4.2.1. Materials

POB was supplied by Ecodiesel Colombia S.A. The POB was prepared from degummed, bleached, and deodorized palm oil and was obtained dynamically from a sampling loop in a distribution line in the processing facility. Diatomaceous earth (CELATOM FW-14) was supplied by EP Minerals, LLC (Reno, NV). Natural silicate (SELECT-FF), neutral bleaching earth (B-80), and acid activated bleaching earth (PERFORM-4000) were supplied by Oil-Dri Corporation of America (Chicago, IL). HPLC grade methanol and dichloromethane were acquired from Alfa Aesar (Ward Hill, MA). A FSG standard mixture was obtained from Matreya, Inc. (Pleasant Gap, PA) and was reported to be >98% pure. The composition of the standard mixtures was 56, 25, and 18%, β sitosteryl, campesteryl, and stigmasteryl glucoside, respectively.

4.2.2. Sample conditioning

The POB was manually agitated for 5 min according to the European Standard EN 12662 to resuspend sediments before withdrawing 400 mL samples. Each sample was placed in a 500 mL bottle and heated for 3 h in a water bath at 80 °C under a dry nitrogen atmosphere to erase the thermal history of the sample. This temperature was selected for this step because 40 °C was found unsuitable to redissolve the sediments. Each sample was then allowed to stand for 24 h at 25 °C before treatment with an adsorbent.

4.2.3. Adsorbent treatment

The POB was treated with one of four adsorbents: diatomaceous earth (DE), natural silicate (NS), neutral bleaching earth (NBE), and acid activated bleaching

earth (AABE). Each adsorbent was added to a 400 mL sample of POB and mixed at 250 rpm for 2 h, then filtered through Whatman No. 2 filter paper under vacuum using the filtration apparatus described in the ASTM D7501 Standard Test Method. A bed of adsorbent of approximately 3 cm was formed above the filter paper during the filtration. The time to filter was recorded. The filter and bed of adsorbent were washed with 50 mL *n*-heptane, the *n*-heptane collected after washing was evaporated at 110 °C, and the POB residue was weighed. After filtration, one portion (300 mL) of treated POB was tested for CSFT, as described below. The other portion of treated POB was stored in a 250-mL dark bottle with fluoropolymer resin-lined cap at 25 °C under a dry nitrogen atmosphere. Each treatment was replicated three times.

DE and NS were each tested at two concentrations (1 and 5 mass%) and one temperature (25 °C) in accordance with Tang *et al.* (2010). NBE and AABE were each tested at three temperatures (25, 40, and 110 °C) and one concentration (5 mass%). 110 °C was chosen in accordance with the AOCS Official Method Cc 8b-52 whereas 40 °C was chosen to improve the understanding of the temperature interaction with precipitate absorbance in potential biodiesel refining applications. In the case of bleaching earths, reduced pressure (60 kPa of vacuum) was maintained during all treatments. Samples treated at 40 and 110 °C were heated on a hot plate with manual temperature control, and samples treated at 110 °C were allowed to come to 80 °C before filtration.

4.2.4. Cold soak filtration test

The cold soak filtration test was performed in accordance with the ASTM D7501 Standard Test Method with minor modifications. The filtration proceeded to completion, in contrast to the standard where filtration is stopped after 720 s. The amount of precipitate retained on the glass microfiber filter was determined in accordance with the ASTM D7321 Standard Test Method with minor modifications. After filtration and washing with *n*-heptane, the glass microfiber filter was dried in

an oven at 110 °C for 30 min, in contrast to the standard where the drying temperature is 90 °C. The precipitate content was calculated from the increase in the mass of the glass microfiber filter and was reported in mg L⁻¹.

4.2.5. Biodiesel analysis

The as-received POB and samples collected after filtration through the bed of adsorbent and the Whatman No. 2 filter paper were analyzed to examine the effect of adsorbent treatment on several ASTM D6751 biodiesel properties. Total glycerin was quantified by the SafTest (MP Biomedicals, LLC., Solon, OH) according to the manufacturer's recommendations. Reagents in the SafTest cleave molecules of mono-, di-, and triglycerides. The resulting glycerin is digested enzymatically, and the break down product is measured spectrophotometrically at 570 nm (Lin *et al.*, 2011). Moisture content was determined with a Karl Fischer coulometric titrator DL32 (Mettler Toledo, Columbus, OH) following the ASTM D6304 Standard Test Method. Oxidative stability index (OSI) was determined with a six-channel Oxidative Stability Instrument (Omnion Inc., Rockland, MA) following the AOCS Official Method Cd 12b-92 at 110 °C. Analyses were all performed twice for each replicate of treated biodiesel.

4.2.6. Steryl glucosides analysis

Centrifugation near the POB cloud point temperature was used to concentrate FSG for quantification. 30 mL of biodiesel was centrifuged at 4,300 x g for 60 min at 15 °C. The supernatant was decanted, and the tubes were inverted on paper towels for 30 min to remove any excess biodiesel from the tubes. Tubes containing untreated POB yielded a visible pellet after centrifugation, but a visible pellet was often not observed among adsorbent treatments. Vacuum distillation (150-175 °C, 98 kPa of vacuum, 190 min) confirmed that the amount of FSG remaining in the supernatant was below our limits of detection (25 mg L⁻¹), and therefore centrifugation isolated the FSG in the pellet. Working in a cold room to minimize evaporation of dichloromethane, 0.5 mL of dichloromethane/methanol (2/1, v/v)

was added to the sample tube. The tubes were capped and stored at 25 °C for 15 min and were resuspended with occasional vortexing. After 15 min, samples were centrifuged for 30 s at 4,300 x g and 15 °C to concentrate the FSG on the tube bottom. The samples were filtered through 0.45 µm nylon filters directly into vials for HPLC FSG analysis as reported by Haagenson *et al.* (2014). Before filtration, the sample arising from the centrifuged untreated POB was diluted 1/10 with dichloromethane/methanol (2/1, v/v) to bring the FSG content within the range of the calibration equation. The sample arising from the centrifuged treated biodiesel, in contrast, was not diluted because of the suspicion that it had very low FSG content. ELSD detectors are well known to have a limited range of non-linear concentration response. Thus, concentrations ranging from 100-300 mg L⁻¹ were chosen to achieve a standard curve with good linearity. The parameters of the standard curve were obtained by fitting the experimental data points to a linear equation, resulting in the calibration equation:

$$y = 178336x - 1E^7 \quad (7)$$

where y is the peak area (mV min) and x represents the analyte (FSG) concentration (mg L⁻¹)

4.2.7. Statistical analysis

Data were analyzed by ANOVA followed by the Tukey test for multiple comparisons using Statgraphics Centurion software (free trial version, StatPoint Technologies, Inc., Warrenton, VA). A p -value of less than 0.05 was considered statistically significant.

A two-factor, five-level CCD was conducted to examine the combined effect of adsorbent concentration and contact time on CSFT. CCD consists of the standard 2^k factorial points, a replicated center point, and $2k$ points fixed axially at a

distance from the center given by the general formula $\alpha = 2^{k/4}$, where k is the number of factors. For two factors, α is equal to 1.414. Five replicates of the center point were used to determine the experimental error and the reproducibility of the data. Thus, a set of 13 treatments including 4 factorial points, 4 axial points, and 1 center point replicated five times was carried out in randomized order to minimize the effects of uncontrolled factors.

The low (-1) and high (+) actual levels of the factors were initially fixed at 1 and 5 mass% for adsorbent concentration, and 30 and 120 min for contact time, respectively. The actual levels of the axial points were calculated using Eq. (1).

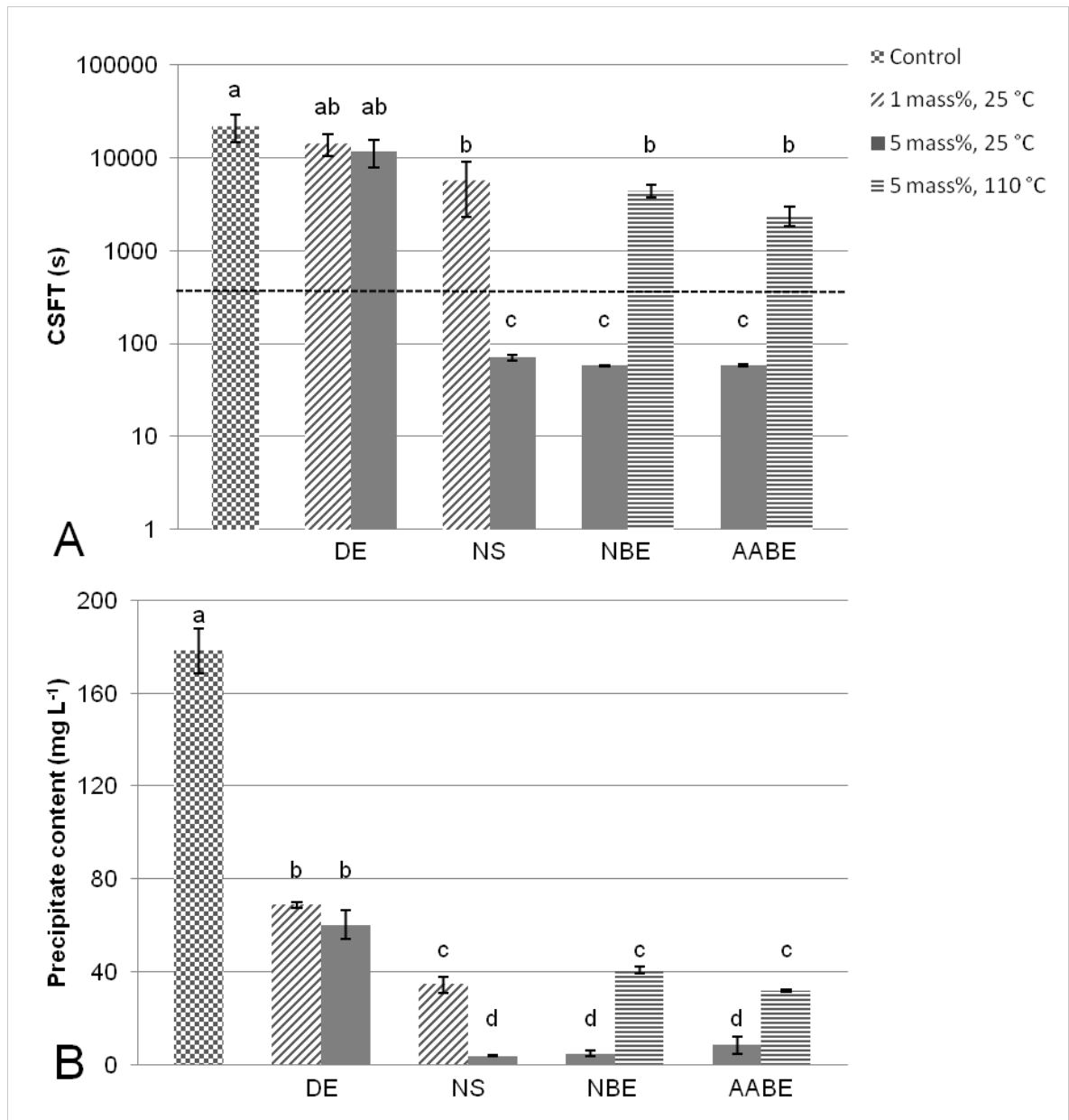
Multiple regression analysis was used to fit the response values by the second-order polynomial model given in Eq. (4). The model was satisfactory when ANOVA showed a high statistical significance (p -value < 0.05). Regression coefficients were also tested for statistical significance. Statgraphics Centurion software (free trial version, StatPoint Technologies, Inc., Warrenton, VA) was employed to determine the regression coefficients and perform the ANOVA. Confirmatory experiments were carried out using 4 combinations of factors that were not part of the original CCD treatments, but within the design space, where favorable CSFT (< 360 s) was expected. The confirmatory experiments involved adsorbent treatment of untreated POB followed by cold soak filtration test of the resulting treated POB as described above.

4.3. RESULTS AND DISCUSSION

Improving POB filterability, through selection of an adsorbent capable of removing the precipitate, was the primary objective of this study. CSFT was markedly higher than the 360 s limit specified in the ASTM D6751 Standard Specification, confirming that POB as received had very poor filterability (Fig. 16A). The precipitate content was also markedly higher in comparison with other biodiesel

feedstocks (Tang *et al.*, 2008b). This indicated that it was necessary to make a great effort to improve POB filterability.

Figure 16. Cold soak filtration time (A) and precipitate content (B) for treated POB. Control denotes the untreated POB. Treatments having different letters are significantly different by Tukey multiple range test (p -value <0.05). The dotted line in A indicates the 360 s ASTM maximum limit for CSFT.



4.3.1. Adsorbent treatment

4.3.1.1. Influence on CSFT

Of the eight adsorbent treatments tested, only three (5 mass% NS, NBE, or AABE at 25 °C) resulted in POB that had a passing CSFT (<360 s) (Fig. 16A). DE was first tested due to its widespread use as a filter aid and its potential use in biodiesel facilities (Lee *et al.*, 2007; Danzer *et al.*, 2011). Although the precipitate content was decreased to almost one-third that of the untreated biodiesel (Fig 16B), the use of either 1 or 5 mass% DE had no significant effect on CSFT. Therefore, additional optimization of DE was not considered.

Using 1 mass% NS, the precipitate content was markedly lower (80.6%) than that for the untreated biodiesel. However, this was insufficient to decrease CSFT to below the ASTM limit. In contrast, using 5 mass%, CSFT decreased to 71 s with a concomitant reduction (97.9%) in the precipitate content. This confirmed that NS can achieve the needed POB filterability.

Effectiveness of bleaching earths on improving POB filterability was then assessed. Since the CSFT was not achieved with DE and NS at 1 mass%, a concentration of 5 mass% was used with bleaching earths. CSFT for POB treated with either NBE or AABE at 25 °C was 58 s, similar to the superior CSFT provided by NS at 5 mass%. The improved CSFT was consistent with a marked reduction (95.3 and 97.3%, respectively) in the precipitate content of both treatments. This suggested the potential of bleaching earths for improving POB filterability. However, the efficacy of bleaching earths on POB precipitate removal and CSFT at 110 °C was decreased. When compared to untreated POB, NBE and AABE tested at 110 °C markedly decreased the precipitate content (77.2 and 82.1%, respectively), but were still higher than that from the bleaching earths tested at 25 °C. These results showed that removal of components responsible for precipitate formation in POB is favored at lower temperature. An explanation for the reduced efficacy at higher temperature may be the alteration in van der Waals physical

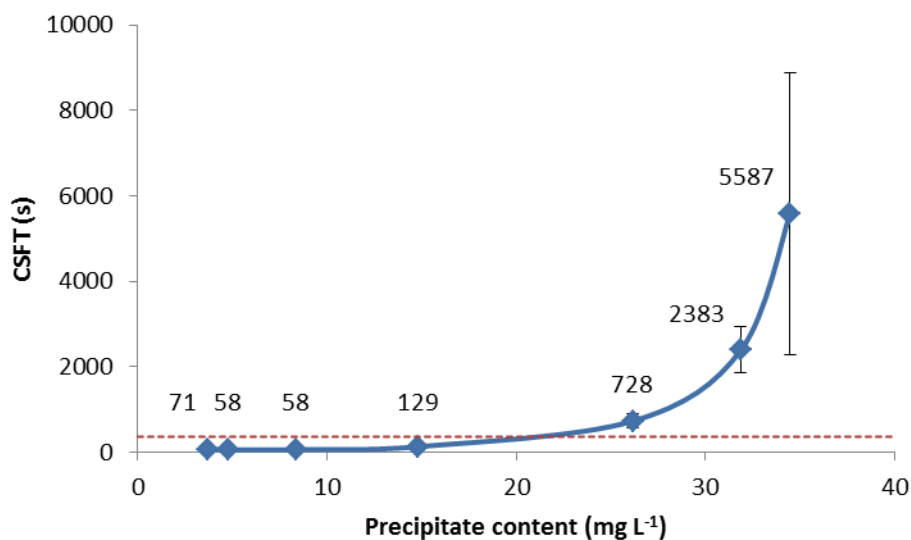
forces at elevated temperature. These forces have been demonstrated to be disrupted when temperature rise, especially above 100 °C, making the adsorption reaction shift to the desorption side (Kaynak *et al.*, 2004). In addition, since the results were not the same at both temperatures, removal of components responsible for precipitate formation in POB by adsorption rather than filtration was supported.

The reduced effectiveness of bleaching earths at increased temperatures was concerning since POB processing often occurs in tropical locations where the average ambient temperature is ≥ 40 °C. Because of this, two additional experiments were conducted at 40 °C to improve the understanding of the temperature interaction with precipitate absorbance in potential biodiesel refining applications. In agreement with our early finding, the precipitate content was higher for the treatments at 40 °C relative to 25 °C, and, consequently, CSFT was also higher. However, the precipitate content at 40 °C were higher for POB treated with NBE than that for POB treated with AABE. Moreover, CSFT for POB treated with NBE was well above the ASTM limit whereas CSFT for POB treated with AABE at 40 °C met the ASTM limit. This suggested the use of AABE instead of NBE for further optimization studies.

As depicted in Figure 17, CSFT increased as the precipitate content rose from 3.68 to 14.44 mg L⁻¹, but still met the ASTM limit. POB failed to meet this limit once the precipitate content exceeded 20 mg L⁻¹. With a further increase in precipitate content, CSFT underwent a sharp rise to very high values beyond the useful range of the ASTM D7501 Standard Test Method. A curve fitted through these data suggests that there is a precipitate content threshold around 20 mg L⁻¹ above which POB filterability becomes unacceptable. A similar relationship was found by Lin *et al.* (2011), who examined the impact of minor components on the precipitate formation in canola oil biodiesel and its filterability. These authors spiked refined canola oil biodiesel with different levels of saturated monoglycerides and tested the

biodiesel for CSFT, quantifying the precipitate content. Their results showed that, below 0.26 mass% saturated monoglycerides, CSFT increased only slightly with increasing precipitate content. However, above this critical point, a small rise in the precipitate content corresponded to a sharp increase in CSFT, at which point the canola oil biodiesel failed to meet the ASTM limit. These authors also mentioned that CSFT was less repeatable once the critical point was exceeded, in accordance with the results reported above.

Figure 17. Relationship between CSFT and precipitate content of POB subjected to different adsorbent treatments. The dotted line indicates the 360 s ASTM maximum limit for CSFT. Only treatments for which precipitate content was lower than 40 mg L⁻¹ (1 and 5 mass% NS at 25 °C; 5 mass% NBE and AABE at 25 and 110 °C) are represented in this plot, including treatments with NBE (precipitate content = 26.2 mg L⁻¹) and AABE (precipitate content = 14.8 mg L⁻¹) at 40°C. Error bars show standard deviation.



Because of the interest in selecting one adsorbent for investigating the effect of adsorbent concentration and contact time on POB filterability in the second part of

this chapter, a criterion was sought to choose between NS and AABE. The amount of POB retained by each spent adsorbent was considered first. However, no significant difference was observed (p -value = 0.5013): NS retained 0.68 ± 0.01 g POB per g adsorbent whereas AABE retained 0.65 ± 0.08 g POB per g adsorbent. The adsorbent price was then considered, and NS cost per ton was almost four times that of AABE. Thus, NS was not evaluated for additional optimization experiments.

4.3.1.2. Influence on minor components content and biodiesel properties

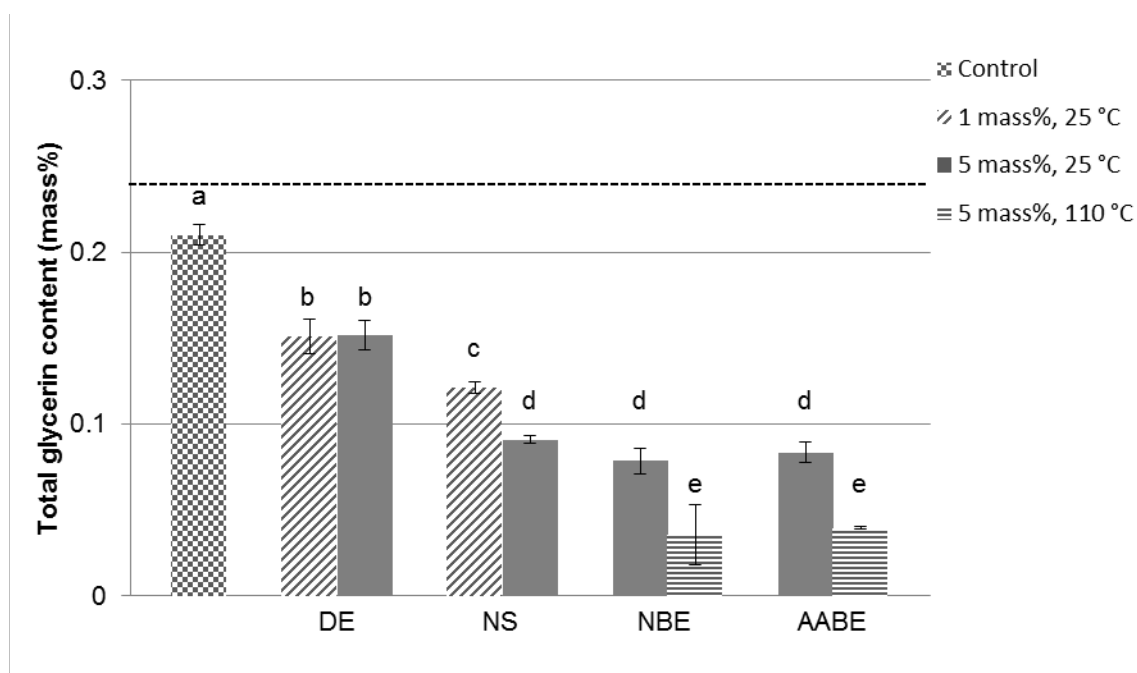
4.3.1.2.1. Total Glycerin

Total glycerin is the sum of free glycerol and glyceride species (mono-, di-, and tri-) remaining in the final biodiesel; of these minor components, monoglycerides are expected to be the most abundant (Dunn, 2006). Since palm oil has a high percentage of saturated fatty acids, the monoglycerides remaining in POB are expected to have a similar, high percentage of saturates. When compared to unsaturated monoglycerides, saturated monoglycerides have been demonstrated to negatively increase CSFT (Lin *et al.*, 2011), and therefore it was expected that reduction in total glycerin content would decrease CSFT of POB.

Adsorbent treatments all markedly decreased the total glycerin content (Fig. 18). However, reduction in total glycerin content did not correspond to a systematic reduction in CSFT (Figs. 16A and 18). Samples treated with either NBE or AABE at 110 °C did not meet the ASTM CSFT limit, despite that total glycerin content for both treatments was the lowest (0.036 and 0.040 mass%, respectively). Although these treatments had the lowest total glycerin content, the precipitate content exceeded the 20 mg L⁻¹ threshold associated with failing CSFT (Fig. 17). The best CSFT was obtained from treatments possessing total glycerin content between 0.078 and 0.091 mass% (5 mass% NS, NBE, or AABE at 25 °C, Figs. 16 and 18), and these treatments had the lowest precipitate content. This suggested that

factors other than saturated monoglycerides, such as FSG, played an important role in POB filterability, in accordance with the results reported in last chapter.

Figure 18. Total glycerin content for treated POB. Treatments having different letters are significantly different by Tukey multiple range test (p -value <0.05). The dotted line indicates the 0.24 mass% ASTM maximum limit for total glycerin content.



4.3.1.2.2. Free steryl glucosides

FSG content of the untreated POB was 65 mg L^{-1} . Samples treated with adsorbent showed a marked reduction in FSG peaks, including no visible FSG peak in some instances. This indicated that all adsorbent treatments decreased the FSG content, even to below our levels of detection (Fig. 19). This was in agreement with Na-Ranong *et al.* (2015), who treated POB containing 97.6 mg L^{-1} FSG at temperatures in the range of $65\text{-}80 \text{ }^\circ\text{C}$ for 10 min and reduced the FSG content to as low as 20 mg L^{-1} using 3 mass% bleaching earths. As suggested above, the superior CSFT of samples treated with 5 mass% NS, NBE, or AABE at $25 \text{ }^\circ\text{C}$ may have been due to a higher reduction in FSG content compared with the other

treatments; this is consistent with Pfalzgraf *et al.* (2007) in their finding that the impact of FSG on soybean oil biodiesel CSFT was the most dramatic, much more dramatic than that of saturated monoglycerides.

Figure 19. Reverse phase HPLC-ELSD chromatogram of centrifuged untreated (A), and centrifuged treated (25 °C and 5 mass% AABE) POB (B). Peaks detected in the range of 5.8-8.2 min corresponded to FSG while in the range of 2.2-3.1 min corresponded to monoglycerides (MG) and in the range of 4.0-5.5 min corresponded to fatty acid esters (FAME) of residual POB. Before analysis, sample A was diluted 1/10 with dichloromethane/methanol (2/1, v/v); sample B, in contrast, was not diluted.

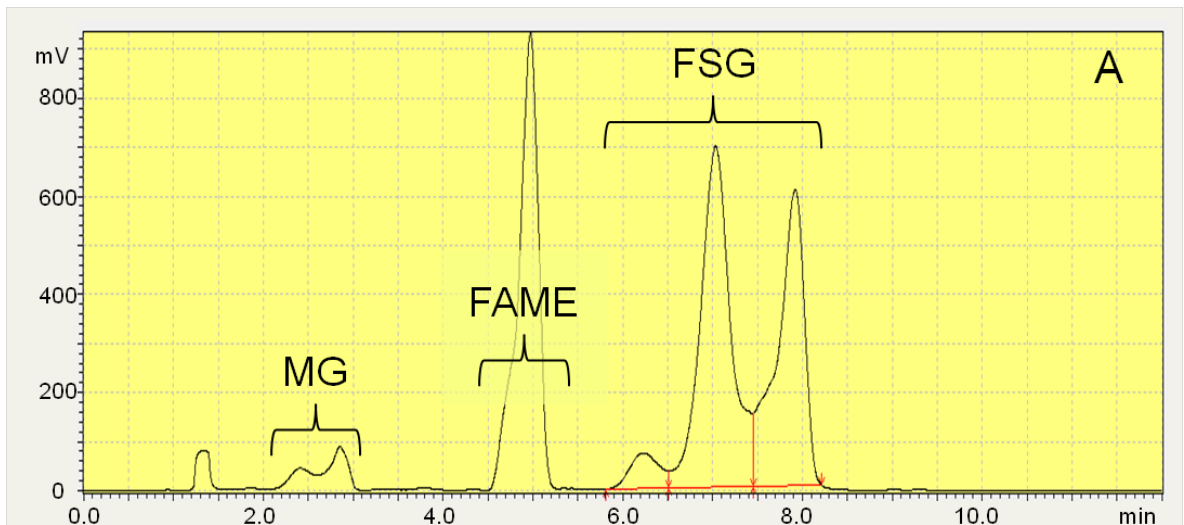
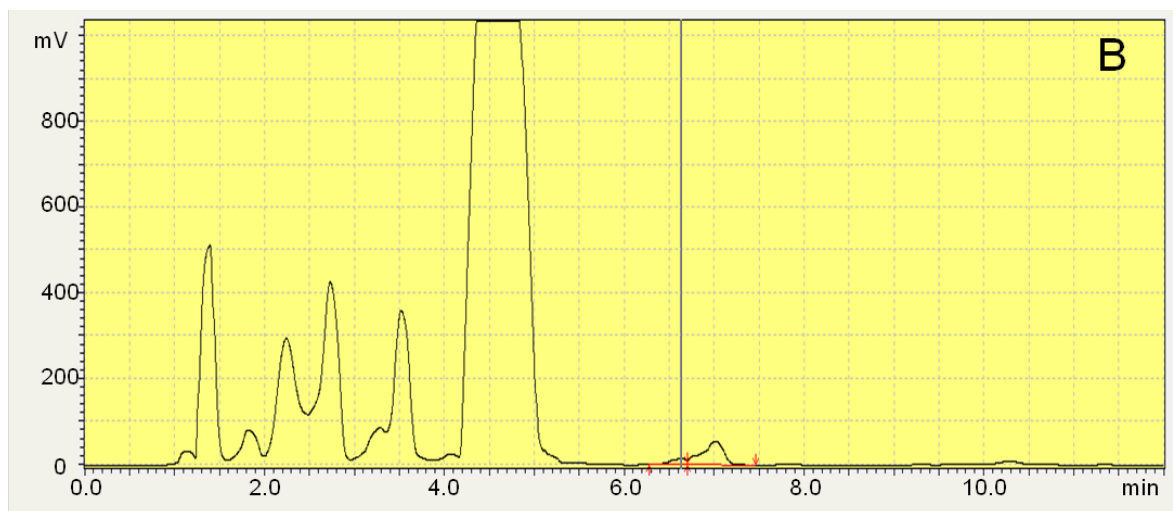


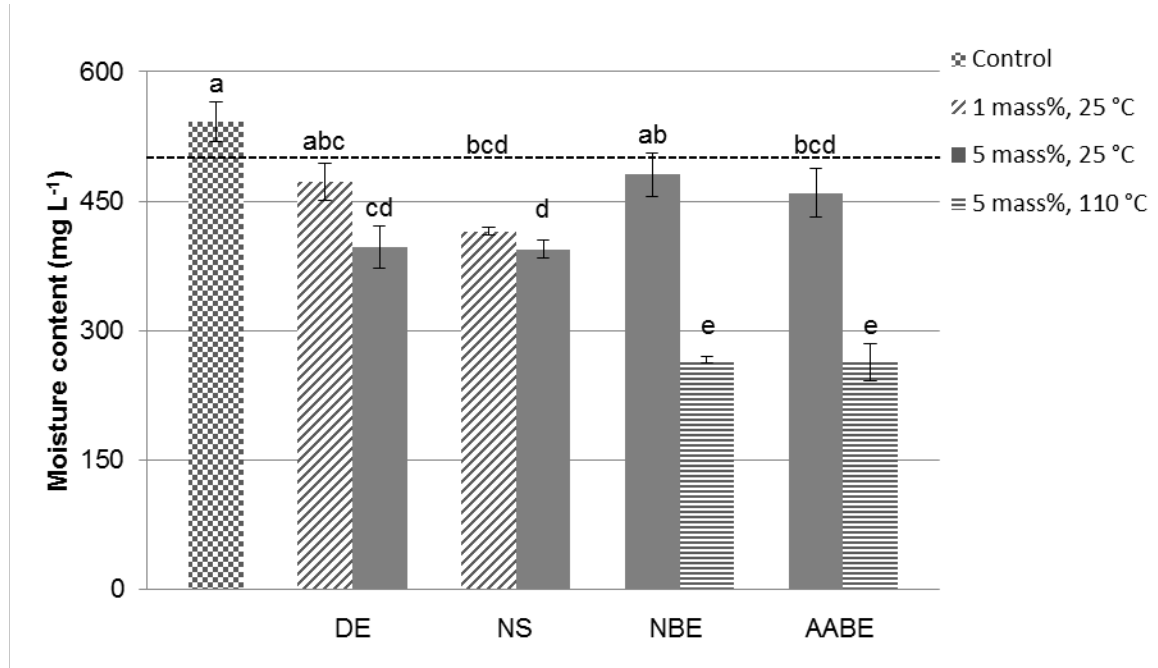
Figure 19. (Continuation)



4.3.1.2.3. Moisture content

Increased biodiesel moisture may negatively impact filtration, and the impact of adsorbent on moisture was determined (Fig. 20). Moisture content for the untreated POB (542.3 mg L^{-1}) was slightly higher than the EN 14214 limit, but all samples treated with adsorbent met this limit. The samples possessing superior CSFT (5 mass% NS, NBE, or AABE at 25 °C, Figs. 16A and 20) had similar moisture contents to the sample treated with 5 mass% DE or the untreated POB, revealing that moisture alone has no significant effect on CSFT. Samples treated with bleaching earths at 110 °C had markedly decreased moisture content. The elevated temperature (110 °C) may have contributed to evaporative loss rather than contact with adsorbent.

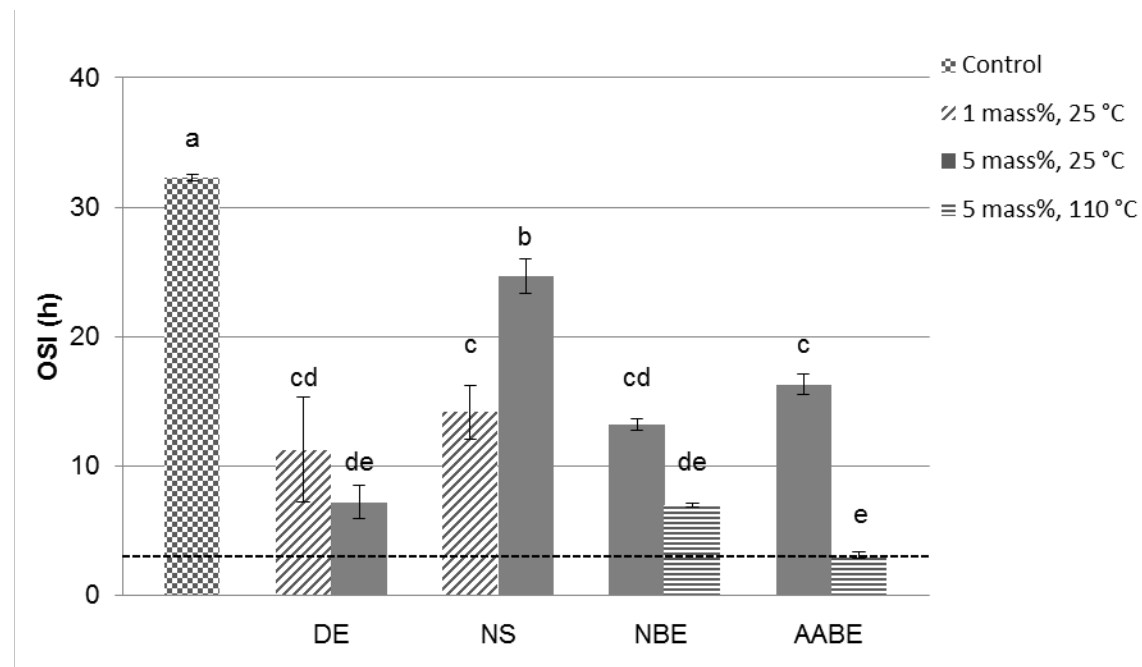
Figure 20. Moisture content for treated POB. Treatments having different letters are significantly different by Tukey multiple range test (p -value <0.05). The dotted line indicates the 500 mg L^{-1} EN 14214 maximum limit for moisture content.



4.3.1.2.4. Oxidative stability index

As expected, the untreated POB had a very high OSI value, well above the 3 h limit specified in the ASTM D6751 Standard Specification (Fig. 21). The high oxidative stability of the untreated POB may be attributed to its high percentage of saturated fatty acids. Biodiesel is more susceptible to oxidation if it contains a high level of unsaturated fatty acids, especially methyl linolenate (McCormick *et al.*, 2007), which is present in POB at trace levels, as reported in chapter II. In addition, POB has natural antioxidants that impart high oxidative stability to biodiesel (Fröhlich and Schober, 2007).

Figure 21. OSI value for treated POB. Treatments having different letters are significantly different by Tukey multiple range test (p -value <0.05). The dotted line indicates the 3 h ASTM minimum limit for OSI value.



All the adsorbent treatments markedly decreased the OSI value compared to the untreated POB, but all samples met the ASTM limit. Biodiesel treated with DE (5 mass%) or with either NBE or AABE at 110 °C had the largest reduction in oxidative stability. Although antioxidant contents were not quantified in this current study, the reduction in OSI may be partly attributed to the removal of antioxidants. Tang *et al.* (2010) reported that adsorbent treatment decreased the soybean oil biodiesel tocopherol content from 36 to 17 mg L⁻¹ on average. These authors suspected that this reduction in the tocopherol content was enough to compromise the soybean oil biodiesel oxidative stability. However, in our case, OSI values remained well above the ASTM limit for treatments for which CSFT was the best (5 mass% NS, NBE or AABE at 25 °C, Figs. 16A and 21), and therefore POB thus treated had not only very good filterability but also very good oxidative stability.

4.3.2. Model fitting

After choosing AABE over NBE and NS for optimization studies, an initial CCD experiment was conducted to examine the combined effect of adsorbent concentration and contact time on CSFT (Table 16). Disappointingly, little variation in CSFT was observed, and all but one treatment decreased CSFT to well below the ASTM limit. The exception was the treatment at 0.18 mass% and 75 min, for which CSFT remained exceptionally high (>1800 s). No statistically significant variation was observed within the design space, indicating that AABE was capable of effectively improving POB filterability even at 1 mass% and 30 min. These results suggested that acceptable POB filterability might be achieved using less than 1 mass% and less than 30 min. Thus, a second CCD experiment was conducted with lower levels of adsorbent concentration and contact time in order to provide a more sound statistical basis for adsorbent loading and retention time (Table 16).

Table 16. Two central composite designs examining the effect of AABE concentration and contact time on CSFT of POB.

Treatment	First CCD			Second CCD		
	Conc. (mass%)	Time (min)	CSFT (s)	Conc. (mass%)	Time (min)	CSFT (s)
1	1 (-1)	30 (-1)	67	0.3 (-1)	10 (-1)	1878
2	5 (+1)	30 (-1)	57	0.9 (+1)	10 (-1)	106
3	1 (-1)	120 (+1)	68	0.3 (-1)	30 (+1)	729
4	5 (+1)	120 (+1)	59	0.9 (+1)	30 (+1)	88
5	0.18 (- α)	75 (0)	1882	0.18 (- α)	20 (0)	1335
6	5.83 (+ α)	75 (0)	56	1.02 (+ α)	20 (0)	59
7	3 (0)	11 (- α)	61	0.6 (0)	6 (- α)	236
8	3 (0)	139 (+ α)	54	0.6 (0)	34 (+ α)	140
9	3 (0)	75 (0)	58	0.6 (0)	20 (0)	322
10	3 (0)	75 (0)	59	0.6 (0)	20 (0)	398
11	3 (0)	75 (0)	59	0.6 (0)	20 (0)	273
12	3 (0)	75 (0)	58	0.6 (0)	20 (0)	263
13	3 (0)	75 (0)	58	0.6 (0)	20 (0)	322

The adsorbent concentration values in the second CCD experiment were chosen so that the highest and lowest axial values equaled the lowest factorial value (1 mass%) and lowest axial value (0.18 mass%) of the first CCD experiment, respectively. Additional adsorbent concentrations values were calculated using Eq. (2) and (3). The new contact time values were chosen in accordance with Barrios and Skelton (2008), who examined the efficiency of magnesium silicate for removal of methanol, glycerin, and fatty acid soaps from used cooking oil-based biodiesel.

The response values from the second CCD experiment supported that acceptable POB filterability could be achieved using less than 1 mass% and less than 30 min. All center point treatments, with the exception of treatment 10, produced biodiesel that met the ASTM limit using just 0.6 mass% and 20 min.

The response values reported in Table 16 were fitted to the second-order polynomial model described in Eq. (3) using multiple regression analysis. According to the ANOVA results, most coefficients were statistically significant, except for x_2 and x_2^2 (p -value >0.05). The latter was removed from the model, but the former was kept due to the significance of the interaction term x_1x_2 . The resulting model, after excluding the insignificant terms, is given in Eq. (8):

$$CSFT = 3847.34 - 7043.03x_1 - 72.83x_2 + 94.25x_1x_2 + 2833.94x_1^2 \quad (8)$$

where x_1 and x_2 denote adsorbent concentration (mass%) and contact time (min), respectively. The model was statistically significant (p -value = 0.0003). The goodness of fit was evidenced by the high coefficient of determination of the model ($R^2 = 0.9886$), indicating that the model may be used for prediction within the design space with high precision.

Good agreement was shown to exist between the predicted CSFT values and the measured values from confirmatory experiments (Table 17). No marked

differences were observed, and the average deviation was 6.3%. This validated the model given in Eq. (8) within the design space.

Table 17. Confirmatory experiments to validate the regression model prediction for CSFT of treated POB, given AABE concentration and contact time. Adsorption temperature: 25°C.

Concentration (mass%)	Time (min)	CSFT (s)		
		Predicted	Measured	Deviation (%)
0.63	25	199	197	0.86
0.6	20	316	281	11.12
0.66	10	327	297	9.22
0.47	30	307	319	3.86

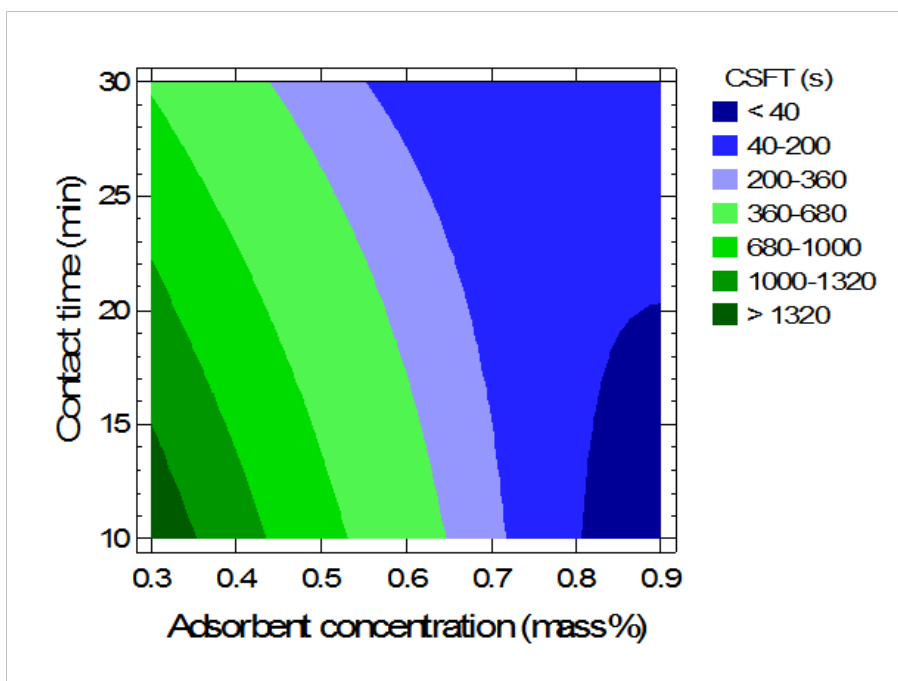
4.3.3. Effect of adsorbent concentration and contact time

Adsorbent concentration had a much larger effect on CSFT than contact time within the ranges used in the second CCD experiment. CSFT varied from values well below the ASTM limit (106 s for treatment 2 and 88 s for treatment 4) to values unacceptably high (1878 s for treatment 1 and 729 s for treatment 3) when adsorbent concentration decreased from 0.9 to 0.3 mass%. The effect of adsorbent concentration was less pronounced at high contact times: CSFT increased by 641 s when adsorbent concentration decreased from 0.9 to 0.3 mass% and contact time was held at 30 min in comparison with 1772 s when adsorbent concentration decreased by the same amount and contact time was held at 10 min, confirming the strong interaction between the adsorbent concentration and contact time. Thus, when decreasing adsorbent concentration, contact time should increase to ensure that CSFT limits are met.

To illustrate the relationship between adsorbent concentration and contact time, a contour plot was created (Fig. 22). The region where CSFT was predicted to be lower than 360 s extends from 0.65 up to 0.9 mass% for adsorbent concentration at the lowest level contact time. This indicates that any combination of adsorbent at ≥ 0.65 mass% and 10 min should decrease CSFT to below 360 s. Lower

concentrations (up to 0.44 mass%) could be effective, but increasing the contact time up to 30 min would be necessary.

Figure 22. Contour plot for the combined effect of adsorbent concentration and contact time on CSFT for treated POB. The ASTM D6751 Standard Specification stipulates that CSFT should not exceed 360 s. In some instances, a more stringent limit of 200 s is used.



The ASTM D6751 Standard Specification also prescribes that biodiesel intended for blending into diesel in cold climates (at or below -12 °C) should have a CSFT of ≤ 200 s. Thus, the region where CSFT was predicted to be lower than 200 s was also identified in the contour plot. Any combination of ≥ 0.72 mass% of adsorbent and 10 min was sufficient enough to decrease CSFT to below 200 s. Again, lower adsorbent concentrations could be effectively used (up to 0.55 mass%), but it would be necessary to increase the contact time up to 30 min.

It is important to note that the improved filtration values were obtained from an untreated biodiesel feedstock containing 65 ppm FSG. FSG content of biodiesel may vary markedly depending on the oil refining processes and the biodiesel production processes (Tang *et al.*, 2010). It may range from 55 to 275 ppm for POB (Van Hoed *et al.*, 2008). Thus, the biodiesel precipitate content may be quite different, and it may be necessary to adjust adsorbent concentrations and contact times for different process batches. In addition, costs associated with the AABE, loss of POB during filtration, and related costs must be taken into account to determine the economic feasibility of the process.

The cost of this treatment was estimated on the assumption that it would be comparable to the cost of bleaching. Morad *et al.* (2010) had reported that 20% of refining cost is due to combined degumming and bleaching, and that the consumption of expensive bleaching agents along with oil losses in the spent bleaching agents make bleaching cost-intensive. In accordance with this and the palm oil's prices reported by the National Federation of Oil Palm Growers (FEDEPALMA) in its publication "Informe Diario de Precios y Mercados", the refining cost for palm oil during the last year was estimated at US\$ 44.02 per ton (2014b); thus, our adsorbent treatment of POB was estimated at US\$ 8.80 per ton.

An estimate of POB losses using 3 mass% AABE may be made from the amount of POB retained by the spent AABE, which was 2.07 ± 0.27 mass%. This value is similar to that reported by Na-Ranong *et al.* (2015) (1.93 mass%). The optimum adsorbent concentration may actually be much lower than 3 mass%, which would reduce both adsorbent cost and POB loss; the optimum for our POB was 0.65 mass%, as reported above.

4.4. CONCLUSIONS

POB as-received from Ecodiesel Colombia S.A. was characterized by an exceptionally high CSFT (>5 h), confirming the poor filterability typical of POB. This was consistent with a high precipitate content (>175 mg L⁻¹), much higher than for biodiesel from other feedstocks. Reduction of the precipitate content to below 20 mg L⁻¹ resulted in POB that had a passing CSFT (<360 s). DE was not successful in improving POB filterability. In contrast, NS, NBE, and AABE achieved the needed filterability at 5 mass% and 25 °C. AABE was selected for optimization because of its cost and its better performance at room temperatures. The improvement in filterability was diminished at higher temperatures, perhaps because of the alteration in van der Waals physical forces at elevated temperature.

All adsorbent treatments significantly decreased the total glycerin content and moisture content. Reduction in total glycerin content did not correspond to a systematic reduction in CSFT, confirming that factors other than saturated monoglycerides played an important role in POB filterability. The OSI value was also decreased, but it remained above the ASTM limit.

A model for the prediction of CSFT of POB, given AABE concentration and contact time, had high statistical significance (*p*-value = 0.0003). The combination of 0.65 mass% AABE and 10 min at 25 °C decreased CSFT to below the ASTM limit. Lower adsorbent concentrations could be effective down to 0.44 mass%, given a corresponding increase in the contact time up to 30 min.

5. GENERAL CONCLUSIONS AND RECOMMENDATIONS FOR FUTURE RESEARCH

The findings from this research provided crucial information about the nature of precipitates formed in POB and the influence of minor components on precipitate formation and filterability of POB. Precipitates were demonstrated to be mostly composed of FSG and monoglycerides, especially monopalmitin, along with ASG and fatty acid soaps. This resulted in the development of a technique to improve POB filterability not only focused on the removal of FSG from POB. AABE for adsorbent treatment of POB was chosen over other three commercial adsorbents (DE, NS, and NBE), and operational conditions of treatment with AABE were further optimized. The combination of 0.65 mass% AABE and 10 min at 25°C decreased CSFT to below the ASTM limit. In addition, POB treated with adsorbent had not only very good filterability but also very good oxidative stability.

The precipitate content increased with increasing FSG content, and this effect was more pronounced at high moisture contents. However, the precipitate content decreased with increasing monoglycerides content. It was conjectured that smaller-sized precipitate may have been formed at high levels of monoglycerides, and this precipitate may have been less retained on the glass microfiber filter. Further research could be carried out in the future to improve the understanding of the interaction of minor components with size and shape of precipitate, and its thermal behavior as well. Such research may include: a) isolation and purification of precipitate formed under controlled conditions in POB, b) examination of morphology and thermal profile of the precipitate using techniques such as SEM and DSC. Interaction between minor components may result in several phases of precipitate possessing different size, shape, and solubility (Chupka *et al.*, 2012).

As noted in chapter I, mandatory blends of diesel and biodiesel are currently used throughout the Colombian territory, and it is expected that biodiesel demand will

expand to B20 blend by 2020 (Rincón *et al.*, 2015). Therefore, it could be crucial to investigate the influence of blending with diesel on precipitate formation and filterability of POB. More precipitate may be formed as a result of blending with diesel in comparison with pure biodiesel (Tang *et al.*, 2008b). This “solvency effect” is due to polarity differences between precipitate and the bulk medium where precipitate is immersed. As the level of biodiesel decreases, the bulk medium polarity decreases as well, thereby causing more precipitate to be formed and the solubility barrier imposed by the bulk medium polarity to be overcome easily (McGinnis and Peyton, 2010). Thus, it may be necessary to adjust adsorbent concentrations and contact times for adsorbent treatment of POB intended for blending with diesel. Such research may include: a) analysis of blends of diesel and POB for CSFT and the precipitate content, b) optimization of operational conditions of adsorbent treatment of POB intended for blending with diesel.

REFERENCES

AGUIRRE Andrés, PEIRU Salvador, EBERHARDT Florencia, VETCHER Leandro, CABRERA Rodolfo, MENZELLA Hugo G. Enzymatic Hydrolysis of Steryl Glucosides, Major Contaminants of Vegetable Oil-Derived Biodiesel. In: Appl Microbiol Biotechnol, 2014, 98:4033-4040.

ALLEMAN Teresa L, MCCORMICK Robert L. Results of the 2007 B100 Quality Survey [online]. <http://www.nrel.gov/docs/fy08osti/42787.pdf> [accessed Mar 2013].

AMERICAN SOCIETY FOR TESTING AND MATERIALS. Standard Specification for Biodiesel Fuel Blend Stock (B100) for Middle Distillate Fuels. In: Annual Book of ASTM Standards. West Conshohocken, PA: ASTM International, 2012. Method D6751.

AMERICAN SOCIETY FOR TESTING AND MATERIALS. Standard Test Method for Cloud Point of Petroleum Products. In: Annual Book of ASTM Standards. West Conshohocken, PA: ASTM International, 2012. Method D2500.

AMERICAN SOCIETY FOR TESTING AND MATERIALS. Standard Test Method for Determination of Fuel Filter Blocking Potential of Biodiesel (B100) Blend Stock by Cold Soak Filtration Test (CSFT). In: Annual Book of ASTM Standards. In: Annual Book of ASTM Standards. West Conshohocken, PA: ASTM International, 2012. Method D7501.

AMERICAN SOCIETY FOR TESTING AND MATERIALS. Standard Test Method for Determination of Total Monoglycerides, Total Diglycerides, Total Triglycerides, and Free and Total Glycerin in B-100 Biodiesel Methyl Esters by Gas Chromatography. In: Annual Book of ASTM Standards. West Conshohocken, PA: ASTM International, 2012. Method D6584.

AMERICAN SOCIETY FOR TESTING AND MATERIALS. Standard Test Method for Determination of Water in Petroleum Products, Lubricating Oils, and Additives by Coulometric Karl Fischer Titration. In: Annual Book of ASTM Standards. West Conshohocken, PA: ASTM International, 2012. Method D6304.

AMERICAN SOCIETY FOR TESTING AND MATERIALS. Standard Test Method for Distillation of Heavy Hydrocarbon Mixtures (Vacuum Potstill Method). In: Annual Book of ASTM Standards. West Conshohocken, PA: ASTM International, 2012. Method D5236.

AMERICAN SOCIETY FOR TESTING AND MATERIALS. Standard Test Method for Particulate Contamination of Biodiesel B100 Blend Stock Biodiesel Esters and Biodiesel Blends by Laboratory Filtration. In: Annual Book of ASTM Standards. West Conshohocken, PA: ASTM International, 2012. Method D7321.

AMERICAN SOCIETY FOR TESTING AND MATERIALS. Standard Test Method for Water Using Volumetric Karl Fischer Titration. In: Annual Book of ASTM Standards. West Conshohocken, PA: ASTM International, 2012. Method E203.

ATABANI Abdelaziz Emad, SILITONGA Arridina Susan, BADRUDDIN Irfan Anjum, MAHLIA Teuku Meurah Indra, MASJUKI Hassan Hassan, MEKHILEF Saad. A Comprehensive Review on Biodiesel as an Alternative Energy Resource and its Characteristics. In: Renewable Sustainable Energy Rev, 2012, 15:1937-1949.

ATADASHI IM, AROUA Mohamed Kheireddine Heireddine, ABDUL AZIZ Abdul Aziz. High Quality Biodiesel and its Diesel Engine Application: A Review. In: Renewable Sustainable Energy Rev, 2010, 14:1999-2008.

BERRIOS Mónica, SKELTON Robert L. Comparison of Purification Methods for Biodiesel. In: Chem Eng J, 2008, 144:459-465.

BONDIOLI Paolo. Nature of Some Insoluble Materials Recovered from Biodiesel Samples. In: Eur J Lipid Sci Technol, 2009, 111:814-821.

BONDIOLI Paolo, CORTESI Nicoletta, MARIANI Carlo. Identification and Quantification of Steryl Glucosides in Biodiesel. In: Eur J Lipid Sci Technol, 2008, 110:120-126.

BRASK Jesper, NIELSEN Per Munk. Enzymatic Removal of Steryl Glycosides in Fatty Acid Alkyl Esters. U.S. Application Patent 20120009659, 2012.

CHUPKA Gina M, FOUTS Lisa, MCCORMICK Robert L. Effect of Low-Level Impurities on Low-Temperature Performance Properties of Biodiesel. In: Energy Environ Sci, 2012, 5:8734-8742.

CHUPKA Gina M, YANOWITZ Janet, CHIU Gordon, ALLEMAN Teresa L, MCCORMICK Robert L. Effect of Saturated Monoglyceride Polymorphism on Low-Temperature Performance of Biodiesel. In: Energy Fuels, 2011, 25:398-405.

DANZER Myron Francis, ELY Timothy L, KINGERY Scott Alan, MCCALLEY Wayne William, MCDONALD William Michael, MOSTEK John, SCHULTES Matthew Leonard. Biodiesel Cold Filtration Process. Canada patent 2576750, 2011.

DUNN Robert O. Effects of Minor Constituents on Cold Flow Properties and Performance of Biodiesel. In: Prog Energy Combust Sci, 2009, 35:481-489.

EUROPEAN COMMITTEE FOR STANDARDIZATION. Liquid Petroleum Products. Fatty Acid Methyl Esters (FAME) for Use in Diesel Engines and Heating Applications. Requirements and Test Methods. Brussels: European Committee for Standardization (CEN), 2012. Method EN 14214.

FARAHANI Mohsen, PAGÉ Daniel JYS, TURINGIA MP. Sedimentation in Biodiesel and Ultra Low Sulfur Diesel Fuel Blends. In: Fuel, 2011, 90:951-957.

FEDEPALMA. Experiencia del Gremio Palmero Colombiano en el Desarrollo del Biodiesel de Palma [online]. <http://web.fedepalma.org/node/894> [accessed Dec 2014a].

FEDEPALMA. Indicadores [online]. <http://web.fedepalma.org/> [accessed Dec 2014b].

FERNANDES JÚNIOR Valter José, DE SOUSA ARAUJO António, DA SILVA VINHADO Fábio, PIVESSO Paulo Roberto. Caracterização de Resíduo Sólido Formado em Biodiesel de Sebo Bovino. In: Quim Nova, 2012, 35:1901-1906.

FIRESTONE David. Bleaching Test for Soybean Oil (Refined). In: Official Methods and Recommended Practices of the AOCS. Champaign, IL: AOCS Press, 2013. Official Method Cc 8b-52.

FIRESTONE David. Oil Stability Index (OSI). In: Official Methods and Recommended Practices of the AOCS. Champaign, IL: AOCS Press, 2013. Official Method Cd 12b-92.

FRÖHLICH András, SCHÖBER Sigurd. The Influence of Tocopherols on the Oxidation Stability of Methyl Esters. In: J Amer Oil Chem Soc, 2007, 84:579-585.

GONZALEZ DELGADO Ángel Darío. Development of a Topology of Biorefinery for Obtaining Biofuels and Bioproducts from Microalgae Biomass (dissertation). Bucaramanga: Universidad Industrial de Santander, 2014.

GUTIÉRREZ PULIDO Humberto, DE LA VARA SALAZAR Ramón. Análisis y Diseño de Experimentos. México D.F.: McGraw-Hill Interamericana Editores S.A., 2008. p. 166-235, 338-430.

HAAGENSON Darrin M, PERLEBERG James R, WIESENBORN Dennis P. Fractionation of Canola Biodiesel Sediment for Quantification of Steryl Glucosides with HPLC/ELSD. In: J Am Oil Chem Soc, 2014, 91:497-502.

HOEKMAN S Kent, BROCH Amber, ROBBINS Curtis, CENICEROS Eric, NATARAJAN Mani. Review of Biodiesel Composition, Properties, and Specifications. In: Renewable Sustainable Energy Rev, 2012, 16:143169.

JANSSEN Rainer, RUTZ Dominik Damian. Sustainability of Biofuels in Latin America: Risks and Opportunities. In: Energy Policy, 2011, 39:5717-5725.

KAYNAK G, ERSOZ Mustafa, KARA Hüseyin. Investigation of the Properties of Oil at the Bleaching Unit of an Oil Refinery. In: J Colloid Interface Sci, 2004, 280:131-138.

KNOTHE Gerhard. Analyzing Biodiesel: Standards and Other Methods. In: J Am Oil Chem Soc, 2006, 83:823-833.

KNOTHE Gerhard, VAN GERPEN Jon, KRAHL Jurgen. The Biodiesel Handbook. Champaign, IL: AOCS Press, 2005.

KOTRBA Ron. Bound by Determination [online].
<http://www.biodieselmagazine.com/articles/1179/bound-by-determination>
[accessed Nov 2011].

LACOSTE Florence, DEJEAN Franck, GRIFFON Hugues, ROUQUETTE Charlotte. Quantification of Free and Esterified Steryl Glucosides in Vegetable Oils and Biodiesel. In: Eur J Lipid Sci Technol, 2009, 111:822-828.

LAM Man Kee, TAN Kok Tat, LEE Keat Teong, MOHAMED Abdul Rahman. Malaysian palm oil: Surviving the Food versus Fuel Dispute for a Sustainable Future. In: Renewable Sustainable Energy Rev, 2009, 13:1456-1464.

LEE Inmok, MAYFIELD Jerry, PFALZGRAF Lisa, SOLHEIM Leif, BLOOMER Scoot. Processes of Producing Biodiesel and Biodiesel Produced Therefrom. U.S. Application Patent 20070151146, 2007.

LIANG Yungchee C, MAY Chooyuen Y, FOON Cheng Sit, NGAN MaAh, HOCK Chuah Cheng, BASIRON Yusof. The Effect of Natural and Synthetic Antioxidants on the Oxidative Stability of Palm Diesel. In: Fuel, 2006, 85:867-870.

LIN Hongjian, HAAGENSON Darrin M, WIESENBORN Dennis P, PRYOR Scott W. Effect of Trace Contaminants on Cold Soak Filterability of Canola Biodiesel. In: Fuel, 2011, 90:1771-1777.

LOPES Shailesh Martin, CONRAN Douglas, RUSSELL Michael. Effectiveness of Cold Soak Filtration Test to Predict Precipitate Formation in Biodiesel. In: SAE, 2011, Technical Paper 2011-01-1201.

MCALPIN Casey R, VOORHEES Kent J, ALLEMAN Teresa L, MCCORMICK Robert L. Ternary Matrix for the Matrix-Assisted Laser Desorption Ionization Time-of-Flight Mass Spectrometry (MALDI TOF MS) Analysis of Non-fuel Lipid Components in Biodiesel. In: Energy Fuels, 2011, 25:5407-5415.

MCCORMICK Robert L, RATCLIFF Matthew A, MOENS Luc, LAWRENCE Rod. Several Factors Affecting the Stability of Biodiesel in Standard Accelerated Tests. In: Fuel Process Technol, 2007, 88:651-657.

MCGINNIS Timothy P, PEYTON Kim B. Analytical Characterization of Sediment Formed in Soy Oil-Based B20 Biodiesel. In: J ASTM Int, 2010, 7, paper ID JAI102584.

MEKHILEF Saad, SIGA S, SAIDUR Rahman. A review on Palm Oil Biodiesel as a Source of Renewable Fuel. In: Renewable Sustainable Energy Rev, 2011, 15:1937-1949.

MIRGHANI Mohamed Elwathig Saeed, CHE MAN YB, JINAP Selamat, BAHARIN Badlishah Sham Ham, BAKAR Jamilar. FTIR Spectroscopic Determination of Soap in Refined Vegetable Oils. In: J Am Oil Chem Soc, 2002, 79:111-116.

MORAD Noor Azia, MOHD ZIN Rohani, MOHD YUSOF Khairiyah, ABDUL AZIZ Mustafa Kamal. Process Modelling of Combined Degumming and Bleaching in Palm Oil Refining Using Artificial Neural Network. In: J Am Oil Chem Soc, 2010, 87:1381-1388.

MOREAU Robert A, SCOTT Karen M, HAAS Michael J. The Identification and Quantification of Steryl Glucosides in Precipitates from Commercial Biodiesel. In: J Am Oil Chem Soc, 2008, 85:761-770.

MOSER Bryan R. Influence of Extended Storage on Fuel Properties of Methyl Esters Prepared from Canola, Palm, Soybean and Sunflower Oils. In: Renewable Energy, 2011, 36:1221-1226.

MURUI Tateo, SIEW YH. Effect of Refining Process on the Content of Sterylglycosides and Alcohols in Palm Oil. In: J Jpn Oil Chem Soc, 1997, 46:683-686.

NA-RANONG Duangkamol, LAUNGTHALEONGPONG Pattarin, KHAMBUNG Suttirat. Removal of Steryl Glucosides in Palm Oil Based Biodiesel Using Magnesium Silicate and Bleaching Earth. In: Fuel, 2015, 143:229-235.

NYSTRÖM Laura, SCHÄR Aline, LAMPI Anna Maija. Steryl Glycosides and Acylated Steryl Glycosides in Plant Foods Reflect Unique Sterol Patterns. In: Eur J Lipid Sci Technol, 2012, 114:656-669.

PFALZGRAF Lisa, LEE Inmok, FOSTER James, POPPE George. Effect of Minor Components in Soy Biodiesel on Cloud Point and Filterability. In: Inform Supplement, Biorenewable Resources No. 4. Champaign, IL: AOCS Press, 2007. p. 17-21.

PLATA Vladimir, GAUTHIER-MARADEI Paola, ROMERO-BOHÓRQUEZ Arnold Rafael, KAFAROV Viatcheslav, CASTILLO Edgar. Characterization of Insoluble Material Isolated from Colombian Palm Oil Biodiesel. In: Biomass Bioenergy, 2015, 74:6-14.

PRADA Fausto, AYALA-DIAZ Iván M, DELGADO Wilman, RUIZ-ROMERO Rodrigo, ROMERO Hernán M. Effect of Fruit Ripening on Content and Chemical Composition of Oil from Three Oil Palm Cultivars (*Elaeis guineensis* Jacq.) Grown in Colombia. In: J Agric Food Chem, 2011, 59:10136-10142.

RINCÓN Luis E, VALENCIA Mónica J, HERNÁNDEZ Valentina, MATAALLANA Luis Gerónimo, CARDONA Carlos Ariel. Optimization of the Colombian Biodiesel

Supply Chain from Oil Palm Crop Based on Techno-Economical and Environmental Criteria. In: Energy Econ, 2015, 47:154-167.

RODIER Jean, GEOFFRAY C, KOVACSIK G, LAPORTE J, PLISSIER M, SCHEIDHAUER J, VERNEAUX J, VIAL J, RODI L. Análisis de las Aguas. Barcelona, Spain: Ediciones Omega S.A., 1998. p. 404-409.

ROMAIN Valentin, NGAKEGNI-LIMBILI Adolphe Christian, MOULOINGUI Zéphirin, OUAMBA Jean Maurille. Thermal Properties of Monoglycerides from Nephelium Lappaceum L. Oil, as a Natural Source of Saturated and Monounsaturated Fatty Acids. In: Ind Eng Chem Res, 2013, 52:14089-14098.

SHARMA Yogesh Chandra, SINGH Bhaskar N. Development of Biodiesel: Current Scenario. In: Renewable Sustainable Energy Rev, 2009, 13:1646-1651.

SILVERSTEIN Robert, WEBSTER Francis X, KIEMLE David J. Spectrometric Identification of Organic Compounds. Hoboken, NJ: John Wiley & Sons, 2005. p. 96.

SMITH Will. Biodiesel Purification: Finding the Right Fit [online]. <http://www.biodieselmagazine.com/articles/8462/biodiesel-purification-finding-the-right-fit> [accessed Apr 2014].

SOHLING Ulrich, RUF Friedrich, ORTIZ NIEMBRO Jose Antonio, CONDEMARIN VARGAS Rosalina, BELLO Jorge. Process for Removing Steryl Glycosides from Biodiesel. U.S. Application Patent 20120154723, 2011.

TANG Haiying, DE GUZMAN Rhet C, SALLEY Steven O, NG KY Simon. Comparing Process Efficiency in Reducing Steryl Glucosides in Biodiesel. In: J Am Oil Chem Soc, 2010, 87:337-345.

TANG Haiying, DE GUZMAN Rhet C, SALLEY Steven O, NG KY Simon. Formation of Insolubles in Palm Oil-, Yellow Grease-, and Soybean Oil-Based Biodiesel Blends after Cold Soaking at 4°C. In: J Am Oil Chem Soc, 2008a, 85:1173-1182.

TANG Haiying, SALLEY Steven O, NG KY Simon. Fuel Properties and Precipitate Formation at Low Temperature in Soy-, Cottonseed-, and Poultry Fat-Based Biodiesel Blends. In: Fuel, 2008b, 87:3006-3017.

VAN GERPEN Jon. Biodiesel Processing and Production. In: Fuel Process Technol, 2005, 86:1097-1107.

VAN GERPEN Jon, HE B Brian, DUFF Keegan. Measurement and Control Strategies for Sterol Glucosides to Improve Biodiesel Quality, Year 2 [online]. http://www.webpages.uidaho.edu/niatt/research/Final_Reports/KLK759_N11-01.pdf [accessed Mar 2013].

VAN HOED Vera, ZYAYKINA Nadezhda, DE GREYT Wim, MAES Jeroen, VERHÉ Roland, DEMEESTERE Kristof. Identification and Occurrence of Steryl Glucosides in Palm and Soy Biodiesel. In: J Am Oil Chem Soc, 2008, 85:701-709.

VERECKEN Jeroen, MEEUSSEN Wouter, FOUBERT Imogen, LESAFFER Ans, WOUTERS Johan, DEWETTINCK Koen. Comparing the Crystallization and Polymorphic Behaviour of Saturated and Unsaturated Monoglycerides. In: Food Res Int, 2009, 42:1415-1425.

WANG Huali, TANG Haiying, SALLEY Steven, NG KY Simon. Analysis of Sterol Glycosides in Biodiesel and Biodiesel Precipitates. In: J Am Oil Chem Soc, 2010, 87:215-221.

SCIENTIFIC NOVELTY

The number of published articles is a measure of the impact of the activity of a scientist; publications are science indicators accepted and used by the United Nations Educational, Scientific, and Cultural Organization, UNESCO, and the Departamento Administrativo de Ciencia, Tecnología e Innovación, COLCIENCIAS (Gonzalez Delgado, 2014). Product of this research, 4 original research articles have been published in journals homologated by the Departamento Administrativo de Ciencia, Tecnología e Innovación, COLCIENCIAS, and/or indexed in the international bibliographic database SCOPUS. In addition, 5 presentations were given in 4 international scientific conferences. Detailed list is provided below. Thus, the scientific novelty of this research is evidenced by the number of published articles, the quality of the journals where the articles were published, the numbers of presentations, and the quality of the international scientific conferences where the presentations were given (Gonzalez Delgado, 2014).

Scientific Papers:

Paper	Indexed in Scopus	Homologated by COLCIENCIAS (category)
Plata V , Kafarov V, Castillo E (2012) Improving the Low-Temperature Properties and Filterability of Biodiesel. Chem Eng Trans 29:1243-1248	Yes	Yes (A2)
Plata V , Gauthier-Maradei P, Romero-Bohórquez AR, Kafarov V, Castillo E (2015) Characterization of Insoluble Material Isolated from Colombian Palm Oil Biodiesel. Biomass Bioenergy 74:6-14	Yes	Yes (A1)
Plata V , Gauthier-Maradei P, Kafarov V (2015) Influence of Minor Components on Precipitate Formation and Filterability of Palm Oil Biodiesel. Fuel 144:130-136	Yes	Yes (A1)

Scientific Papers (Continuation):

Paper	Indexed in Scopus	Homologated by COLCIENCIAS (category)
Plata V , Haagenson D, Dağdelen A, Wiesenborn D, Kafarov V (2015) Improvement of Palm Oil Biodiesel Filterability by Adsorption Methods. J Am Oil Chem Soc 92:893-903	Yes	Yes (A1)

Conference Papers (Conference Proceedings or Book of Abstracts):

- **Plata V**, Kafarov V, Castillo E. Improving the Low-temperature Properties and Filterability of Biodiesel. 20th International Congress of Chemical and Process Engineering and 15th Conference on Process Integration, Modelling and Optimisation for Energy Saving and Pollution Reduction. ISBN: 978-80-905035-1-9. Prague, Czech Republic, August 25-29, 2012
- **Plata V**, Serrano M, Tiria K, Bohórquez ARR, Kafarov V, Gauthier-Maradei P, Castillo E. Fractionation and Characterization of Insolubles Formed in Palm Oil Biodiesel. 16th Conference on Process Integration, Modelling and Optimization for Energy Saving and Pollution Reduction. ISBN: 978-88-95608-26-6. Rhodes, Greece, 29 September 29-October 2, 2013
- **Plata V**, Gauthier-Maradei P, Kafarov V, Castillo E, Ortiz C. Influence of Minor Components on Haze Formation in Palm Oil Biodiesel. 8th Conference on Sustainable Development of Energy, Water and Environment Systems. ISSN: 1847-7178. Dubrovnik, Croatia, September 22-27, 2013

Other Contributions:

- **Plata V**, Haagenson D, Dağdelen A, Wiesenborn D, Kafarov K. Improvement of Palm Oil Biodiesel Filterability by Adsorption Methods. 2014 American Society of Agricultural and Biological Engineers Intersectional Meeting. Brookings, USA, March 28-29, 2014

- Dağdelen A, Haagenson D, **Plata V**, Wiesenborn D. Isolating and Quantifying Steryl Glucosides from Palm Oil Biodiesel. 2014 American Society of Agricultural and Biological Engineers Intersectional Meeting. Brookings, USA, March 28-29, 2014